

https://dspace.org/

An investigation into the effects of floating objects on the electrical breakdown of air insulation under steady state high voltage direct current conditions

Parus, Nishanth

2015-05-04
http://hdl.handle.net/10539/17607

Downloaded from a DSpace repository. https://dspace.org/

AN INVESTIGATION INTO THE EFFECTS OF FLOATING OBJECTS ON THE ELECTRICAL BREAKDOWN OF AIR INSULATION UNDER STEADY STATE HIGH VOLTAGE DIRECT CURRENT CONDITIONS

NISHANTH PARUS

A research report submitted to the Faculty of Engineering and the Built Environment, University of the Witwatersrand, Johannesburg, in part fulfilment of the requirements for the degree of Master of Science.

Johannesburg, August 2014

Declaration

I declare that this research report is my own, unaided work. It is being submitted in part fulfilment for the Degree of Master of Science at the University of the Witwatersrand, Johannesburg. It has not been submitted before for any degree or examination in any other University.

Signed on August 25, 2014

_____

Nishanth Parus

Student Number: 419443

Abstract

In South Africa, live work is routinely performed on high voltage apparatus at various voltages up to 400 kV ac. With regard to HVDC, there are unqualified parameters relating to the development of the safe live work standards, which are currently based on extrapolation of ac and transient voltage test data. Furthermore, it is generally accepted that the mechanism for air breakdown under dc is different when compared between ac and dc voltage.

The air breakdown mechanism under HVDC conditions and the corresponding live work related parameters need to be researched further before live work may be performed. Experimentation using floating objects, has in the past, been used to study parameters related to live working calculations.

This research report presents the results of HVDC air breakdown tests using a 300 mm diameter floating metallic sphere with a 30 mm protrusion, in a point-to-plane configuration with a total gap length ranging between 0.75 m and 1.4 m. Both positive and negative polarity cases were tested. The results indicated that the position of the floating sphere does not significantly affect the flashover-voltage magnitude. There is, however, a definite reduction in the strength of the air gap, between 27 % and 29 %, for the cases tested. Further, the static charge on the floating object did not influence the breakdown voltage. There is also linearity in the air breakdown voltages of simple point-to-plane air gaps. Humidity and temperature also contribute to variations in the breakdown voltage.

Two international publications have been published based on the research presented in this report. These are listed in Appendix D and E, respectively.

Acknowledgements

Firstly, I would like to thank my parents, Raj and Manju, and my sister Junita for their sacrifice and support for me to complete my studies. This would have not been possible without their encouragement.

I would like to acknowledge Prof. Ian R Jandrell as an invaluable mentor and supervisor. This research is only possible through the opportunity that he has given to me.

I would also like to thank Eskom Holdings SOC Ltd for the financial support of this Masters through the further studies program. I would also like to thank Eskom for the use of the corona cage test facility as well as for the use of the photographs contained herein.

Thanks go to my friends and colleagues Nishal, Thavi, Hinesh, Andreas and Igor who have asked hard questions relating to the research, assistance with the tests and for robust discussion regarding the discharge processes observed.

I would like to acknowledge Riaan Roets and Coenie Esterhuisen for their assistance with developing the test setup and running the tests.

Finally, I am grateful for the blessing and grace of Avdhood Baba Shivanandji, whom has made All this possible and for the greater things to come in the future.

Contents

Page No.

Declaration……i

Abstract……ii

Acknowledgements……iii

Contents……iv

List of Figures……vii

List of Tables……ix

List of Symbols……ix

List of Abbreviations and Acronyms……ix

1. Introduction 1

2. Background 4

2.1 The Southern African Power System Context 4

2.2 Benefits of Live Line Maintenance Work 6

2.3 Issues related to Live Line Work on HVDC Transmission Lines 7

2.3.1 Steady State Voltage versus Impulse Voltage Tests 8

2.3.2 Electrical Breakdown in Air 8

3. Hypothesis and Key Research Questions 13

4. Research Methodology 15

4.1 Simple Rod-to-Plane Breakdown tests 15

4.2 Floating Metallic Sphere Breakdown Tests 15

4.3 Test program 16

4.4 Correction for Standard Temperature and Pressure 17

5. Experimental setup 17

5.1 High Voltage – Direct Current Power Supply 17
5.1.1 Design of the Rectifier 18
5.1.2 Initial Commissioning Tests 21
5.1.3 Voltage Ripple 22
5.2 Simple Point-to-Plane Test Setup 24
5.3 Particulars of the Metallic Sphere 24
5.4 Air Gap Dimensions for the Floating Sphere Tests 26
6. Test Results 27
6.1 Results of the Point-to-Plane Tests 27
6.1.1 Positive Polarity Results 27
6.1.2 Negative Polarity Results 29
6.2 Repeatability of the Breakdown Voltage versus the Gap Size 30
6.3 Results of the Floating Sphere Tests 31
6.3.1 Positive Polarity Case 31
6.3.2 Comparison with the Reference Case 34
6.3.3 Further Images for the Positive Polarity Case 34
6.3.4 Negative Polarity Case 36
6.3.5 Images for the Negative Polarity Tests 37
6.4 Repeatability of the breakdown Voltage versus Gap Size 40
7. Discussion and Analysis 41
7.1 Comparison with Published Literature: Research conducted by Rizk 41
7.2 Limitations of the Power Supply 42
7.3 Leader or Streamer Breakdown Mechanism – Discussion based on Test Observations 42

7.3.1 Analysis of the Negative Polarity Results 43

7.3.2 Analysis of the Positive Polarity Results 44

7.4 The Presence of the Sphere and the Reduction in the Insulation Strength 45

7.5 Altitude Correction 45

7.6 Static Charging of the Floating Object 46

8. Conclusion 47

9. Recommendations 49

10. References 50

11. Appendices 52

11.1 Appendix A: Point-to-Plane Test Results (Positive and Negative Polarity) 52

11.2 Appendix B: Positive Polarity Floating Sphere Test Results 53

11.3 Appendix C: Negative Polarity Floating Sphere Test Results 54

11.4 Appendix D: Publication at ISH 2011 55

11.5 Appendix E: Publication at ISH 2013 62

List of Figures

Figure 1: Overview of potential HVDC development in Southern Africa (Map courtesy of Eskom Holdings SOC Ltd) 5

Figure 2: Live insulator swap-out at reduced voltage on the Cahora Bassa transmission line 6

Figure 3: Spot measurements of PLC telecommunication signal strength 6

Figure 4: Electrostatic discharge between a 400 kV ac line and the live working trolley 8

Figure 5: Glow corona from a conductor (ac voltage) 10

Figure 6: Electron avalanche process (Drawing courtesy Eskom Power Series [15]) 11

Figure 7: 'Floating' live line worker being lowered onto the Cahora Bassa transmission 13

Figure 8: (a) and (b) Examples of live workers being lowered onto ac transmission lines 14

Figure 9: Schematic representation of the test setup 16

Figure 10: Equivalent circuit of the test setup 17

Figure 11: (a) Uncovered original diode stack, (b) Diode covered with silicone rubber sheaths 18

Figure 12: Rectifier mounting platform 19

Figure 13: Hardware rings used around connection points 19

Figure 14: Installation of the diode arrangement in the HV power supply circuit 20

Figure 15: Water resistor and voltage divider 20

Figure 16: Removable display multimeter connected to the ac side of the rectifier 21

Figure 17: CoroCAM® image showing corona discharges on the rectifier 22

Figure 18: Graph showing measured dc voltage 22

Figure 19: Graph showing the ripple measured on the power supply 23

Figure 20: Test setup for the rod-plane experiment 24

Figure 21: Test setup for the floating sphere experiment 25

Figure 22: The sphere used in the tests, showing the 30 mm protrusion 25

Figure 23: Graph showing linearity for positive polarity dc flashover tests 27

Figure 24: (a) and (b) Pictures showing arc behaviour for the positive polarity point to plane tests . 28

Figure 25: Picture showing tortuous arc path at the positive electrode. 28

Figure 26: Picture showing arc initiation a short distance away from the tip of the point electrode.. 29

Figure 27: Graph showing linearity for positive negative dc flashover tests..... 29

Figure 28 (a) and (b): Faint plasma channels observed during the negative polarity tests..... 30

Figure 29: Graph showing the results obtained for the positive polarity between gap sizes ranging from 1 m to 1.4 m (uncorrected data) 31

Figure 30: Graph showing the results obtained for the positive polarity floating object tests (data corrected for STP) 32

Figure 31: Arc attachments for the positive polarity floating object tests, where the sphere was positioned in a location closest to the ground plane 32

Figure 32: CoroCAM® image showing sustained corona discharge at the point electrode. 33

Figure 33: Graph indicating the reduction in insulation strength for the 1 m gap..... 34

Figure 34: Graph indicating the reduction in insulation strength for the 1.25 m gap..... 34

Figure 35: Erratic arc path..... 35

Figure 36: Test image showing the arc evading the sphere 35

Figure 37: CoroCAM® image showing the arc path ignoring the protrusion at the bottom of the sphere 36

Figure 38: Graph showing results for the negative polarity tests (uncorrected for STP) 37

Figure 39: Graph showing results for the negative polarity tests (corrected for STP) 37

Figure 40: Picture showing the arc origination at the bottom of the sphere..... 38

Figure 41: Picture showing discharge activity in the air space between the HV point 38

Figure 42: CoroCAM® images showing (a) sustained discharge activity point and protrusion, and (b) in the air gap between the point and the sphere 39

Figure 43: In figures (a) and (b) above, the heat stress is evident as it distorts the reflection of the cooling fins of the supply transformer, which are normally straight, as shown in (c) 39

Figure 44: Graph of generalised results from [3] 41

Figure 45: Graph indicating the change in linearity between shorter and longer gaps 43

Figure 46: Graph indicating the change in linearity between shorter and longer gaps 44

Figure 47: CoroCAM® images of discharge activity on live working mannequin 46

List of Tables

Table 1: Results of the positive polarity point to plane tests 27
Table 2: Results of the negative polarity point to plane tests 29

List of Symbols

α	Townsend's first ionisation coefficient
°C	Temperature in Degrees Celsius
Ω	Ohm
%	Percent
±	Positive and Negative polarity
p	Gas pressure
R^2	Coefficient of determination
E	Electric field (kV/m or kV/cm)
$x \text{ and } d$	Distance in mm
µ	Micro
µF	Microfarad

List of Abbreviations and Acronyms

A	Ampere
ac	Alternating Current
CT	Current Transformer
dc	Direct Current
EHVDC	Extra High Voltage Direct Current
EPRI	Electric Power Research Institute
HV	High Voltage
HVAC	High Voltage Alternating Current

HVDC	High Voltage Direct Current
IEC	International Electrotechnical Commission
IR	Infrared
km	Kilometre
kPa	Kilopascal
kV	Kilovolt
m	Meter
mA	Milliampere
MAD	Minimum approach distance
mm	Millimetre
ms	Millisecond
MTS	Main Transmission System
MV	Megavolt
MW	Megawatt
NESC	National Electricity Safety Code
OSHA	Occupational Safety and Health Administration
PLC	Power Line Carrier
pF	Pico Farad
pu	Per unit
rms	root mean square
ROF	Risk of Flashover
SAPP	Southern African Power Pool
STP	Standard Temperature and Pressure
uv	Ultraviolet

1. Introduction

Internationally, there are several High Voltage Direct Current (HVDC) schemes in operation, however, only a few of them conduct live work at full nominal voltage. Live line maintenance of such schemes is becoming more important as power utilities are challenged with high availability requirements. As such, the air breakdown mechanism under HVDC conditions, where related to practical live working tower geometries, must be understood before live working may be undertaken.

Worldwide, experience with live work on HVDC transmission lines is limited and little information is available on how minimum approach distance (MAD) values should be determined for HVDC live work. Furthermore, MAD values are based on extrapolations of alternating current (ac) test data and do not account for significant differences between the ac and direct current (dc) flashover characteristics.

This work investigated the influence of a metallic floating sphere on dc breakdown voltage in a point-to-plane test configuration. Floating metallic spheres are often used in experimentation to understand the behaviour of air gaps under high voltage (HV) applications. Substantial information has been published on the electrical breakdown of air gaps [1-3]; however, there is little data available for HVDC at high altitudes and/or large air gaps.

Another important consideration is that the calculations developed for safe live work (whether ac or dc) are primarily based on tests that were done using ac and/or superimposed switching impulse voltages. Such conditions can occur during live work on ac transmission lines and could result in transient over-voltages of up to two (2) per unit (pu) in certain cases [4]. These transient over-voltages occur when circuit breakers on the transmission scheme are operated (i.e. either opened or closed). Circuit breaker operation changes the electrical system by either adding or removing inductance and capacitance. This change to the electrical system causes rapid oscillations in the current and voltages on the interconnected circuits until a new steady state condition is achieved. This type of over-voltage is characterised by heavily damped oscillations with frequencies of up to a several kilohertz. If a live line worker is working on a high voltage apparatus on any of the interconnected circuits, the voltage at the work site will be subject to the travelling transient wave and associated voltage swings. The safe work calculations therefore have to take into account the possibility of transient over-voltages occurring at the work site.

For HVDC, however, there are no circuit breakers on the dc side of the scheme. Over-voltages (e.g. during fault conditions) are minimised by the fast control action of the dc converters. HVDC converters can generally sense and limit fault conditions within a few milliseconds. This control is possible due to the fast switching (typically in the kHz range) of the thyristors or insulated gate bipolar transistors (IGBT's). Alternating current schemes generally take a longer time to recover (usually longer than one cycle – i.e. longer than 20 ms).

Other type of transient over-voltage that could occur on a transmission line is a lightning related transient. A direct lightning strike to the conductor in the case of a shielding failure, a back flashover in the case of a direct strike to a pylon or a strike near the transmission servitude could induce or directly apply such transients onto the line itself, respectively. When compared to switching over-voltages, lightning over-voltages usually have a much steeper wave front and can reach levels up to 10 pu. The resultant travelling wave does, however, decay much quicker as it moves away from the injection point. Live work guidelines [4] do not recommend live work in the presence of lightning or during inclement weather; therefore, the impact of these types of over-voltages are thus limited and lightning impulse tests are not crucial.

Literature published by Manitoba Hydro [5-6] has indicated that line faults have been recorded during fair weather conditions. For these reasons, this research project considered the case of static dc voltage and not transient or temporary over-voltages. Faults at static/steady state conditions may pose a significant risk to live worker and working in this condition needed further research.

It is anticipated that the results obtained from this research may be used in the review of the calculation of MAD for HVDC applications, thereby contributing to a better understanding towards improved safety for live line worker as well as the improvement in live working tool design.

The structure of this report is as follows:

Chapter 2: The main drivers for conducting this research are outlined. Benefits and pitfalls of live work under HVDC are discussed, as well as the purpose for investigating steady state voltage tests instead of transient over-voltages.

Chapter 3: The hypothesis is presented and the key research questions to be answered by this work are listed.

Chapter 4: The methodology of conducting the tests is presented. The reasons and rationale for the test setup and dimensions are discussed.

Chapter 5: Practical issues related to the construction of the experiment are presented. Details pertaining to the specifications and limitations of the test power supply, the floating metallic sphere, the electrodes and the air gap are discussed.

Chapter 6: The results of the tests are documented and a discussion is undertaken.

Chapter 7: Finally, closing remarks and recommendations for further research are noted.

2. Background

2.1 The Southern African Power System Context

The South African ten-year transmission development plan [7], proposed to implement new ±600 kV HVDC schemes within the country. The proposed schemes were to be developed with a high availability requirement in order to ensure a reliable and high quality of supply. Although HVDC schemes have been in existence since the 1950's [8-9]; today, there are still unexplained faults that have been reported. Although new schemes have the benefit of improved design based on the performance and experience from the initial schemes, all risks and unexplained phenomenon that could cause loss of life to live line workers or lead to a dangerous work situation have to be adequately investigated, understood and quantified. Given the high costs of developing transmission schemes, whether ac or dc, it is a techno-economic imperative that these schemes operate near faultless for the maximum period over their useful lifespan. Schemes being proposed in South Africa are to be of the highest achievable reliability, availability and maintainability specifications (i.e. less than one fault per 100 km per year).

The Cahora Bassa scheme is an important link in the South African Main Transmission System (MTS). The South African Power Utility, Eskom, currently operates and maintains the South African section of the Cahora Bassa HVDC scheme. The nominal operating voltage of the scheme is ±533 kV. It accounts for approximately 1600 MW of renewable power, roughly 5% of South Africa's supply capacity [10]. For two reasons, this scheme must be highly reliable:- Firstly, at present, the South African power network does not have surplus generation capacity. The generation fleet is plagued with old equipment, some near to the 'end-of-life' period. Plant outages for repairs are frequent and the MTS cannot tolerate outages of 5% for prolonged periods. Secondly, load rejections of 1600 MW pose a significant risk to the rotating machines at the Cahora Bassa hydro-electric power station. The interlinked Mozambique and Zimbabwe power networks are electrically far too weak to absorb the active power. Any faults on the South African sections of the HVDC transmission line may cause power trips on the Mozambique network, namely, the town of Songo is tripped. Live maintenance to reduce the risk of faults and consequently outages is thus critical to maintaining a stable and reliable South African and Southern African power system.

Figure 1 indicates the potential to import approximately 3500 MW power into the Southern African Power Pool (SAPP) via the Inga River Hydroelectric schemes [11]. The total transmission distance is in excess of 3000 km, making ac transmission unfeasible due to the long line length and the capacitive ac compensation that will be required along the transmission line.

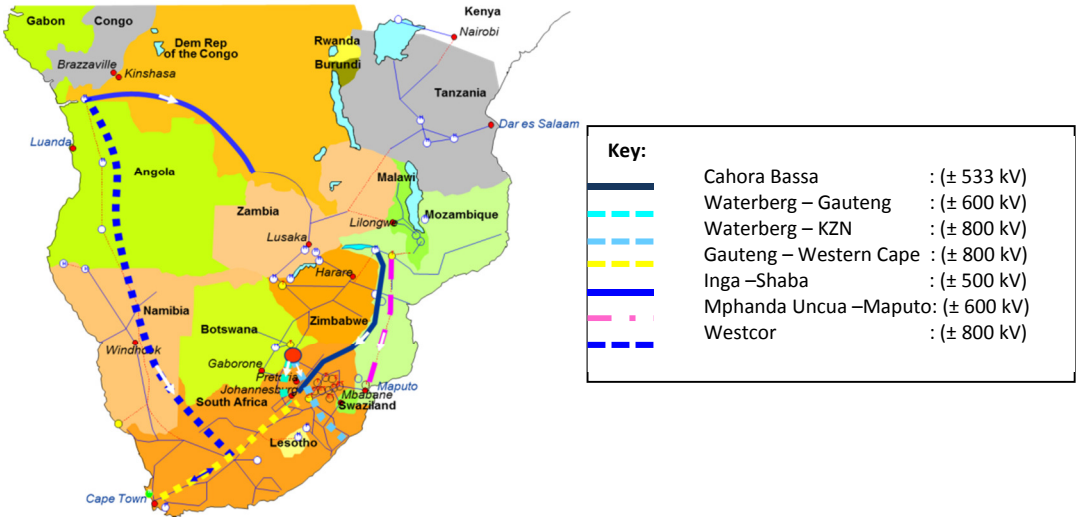


Figure 1: Overview of potential HVDC development in Southern Africa (Map courtesy of Eskom Holdings SOC Ltd)

At the time of writing of this research report, the Mozambican power company Electricidade de Mozambique (EDM) is planning the CESUL project [12], which plans to develop the 1500 MW Mphanda Nkuwa and the 1245 MW Cahora Bassa North Bank hydroelectric power projects. Their transmission backbone plans are to develop ± 500 kV HVDC, 550 kV High voltage alternating current (HVAC) power networks and is projected to interlink SAPP countries.

It is evident that there is significant interest in HVDC and EHVDC transmission schemes. Such proposed schemes have relatively long transmission lines and maintenance of these will be crucial for economic justification of the capital investment for such infrastructure. Technically, the power levels that are being proposed are at the upper limits of current semiconductor technology. Any transmission fault may result in significant load rejections at the hydro-electric (or other) generators. The generator machines should not be subjected to such power swings as it results in a decrease of lifespan of the equipment. Live maintenance is therefore a crucial aspect in the techno-economic justification for HVDC and EHVDC power schemes.

2.2 Benefits of Live Line Maintenance Work

Proactive live maintenance has the potential to reduce plant outages. Experience on ac HV apparatus has shown that live work can be done safely if it is done by suitably trained and qualified lines-men, if proper MAD values are observed and that the voltages at the work site is known and adequately controlled [4]. Literature for HVDC schemes, however, indicates that currently, live work is not being performed at full system voltage [14]. Many utilities prefer to lower the system voltage, thereby decreasing the power throughput, before any live work is done. Uncertainties with the development of the guidelines and standards for HVDC have been cited as the main cause for the requirement to lower the voltage. Figures 2 and 3 indicate examples of where live work can be beneficial to the power utility.

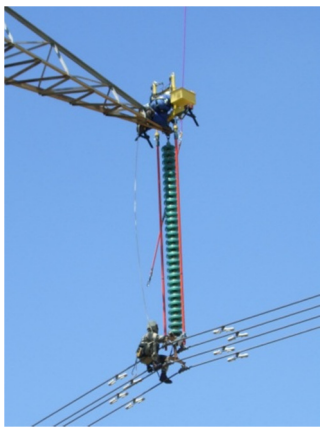


Figure 2: Live insulator swap-out at reduced voltage on the Cahora Bassa transmission line



Figure 3: Spot measurements of PLC telecommunication signal strength

2.3 Issues related to Live Line Work on HVDC Transmission Lines

It is generally accepted that there are differences in the air breakdown mechanism under HVDC conditions to that of HVAC [15]. Factors that influence the dielectric strength include:

- The impact of space charge in the vicinity of the live worker,
- The differences in the air breakdown mechanism for the different polarity dc as well as ac transmission lines,
- The electrical behaviour of a floating object in the air gap,
- The expected temporary and transient over-voltages,
- Correct minimum approach distance (MAD) and risk of flashover (ROF) factors under HVDC and EHVDC conditions.

Several regulatory organisations such as the South African Department of Labour (Occupational Health and Safety Act of 1993) [16], the Occupational Safety and Health Administration (OSHA) and the National Electricity Safety Code® (NESC) have published specifications based on simplified techniques as described in the Institute of Electrical and Electronics Engineers (IEEE) - Standard 516 [17]. While conservative, the approach utilises the equivalent difference between the ac peak and the average dc voltage, based on ac test data. According to the Electric Power Research Institute (EPRI)[14], the values used in the determination of the dc pole-to-pole and pole-to-ground MAD values are based on extrapolations that stretch the applicability of available ac and impulse voltage tests data. This also does not account for significant differences between ac and dc environments. As described above, there are several issues to be considered in the development of a safe live working standard. This research report investigates only one of these issues relating to the behaviour of a floating object in an air gap stressed with dc voltage. As an example of such a case, Figure 4, shows the charge equalisation between a (floating) live work trolley and an energised 400 kV ac line.



Figure 4: Electrostatic discharge between a 400 kV ac line and the live working trolley

2.3.1 Steady State Voltage versus Impulse Voltage Tests

Switching and lightning impulse tests are used to determine flashover characteristics of ac apparatus such as transmission lines. The transient impulses stress the air gap and causes distortions in the electric field greater than the insulation strength of air. Switching impulses are characterised by a waveform with a time to peak of 250 µs and a time to half value of 2500 µs, while lightning impulses are defined by a 1.2 µs by 50 µs waveform, respectively [18]. The time to crest has been shown to have an effect on the flashover-voltage.

For steady state dc, there is no steep fronted voltage waveform that would influence the flashover-voltage. The electro-static fields and the environmental conditions around the test object therefore have a predominant effect on the breakdown.

2.3.2 Electrical Breakdown in Air

At standard temperature and pressure (STP) i.e. 20°C and 101 kPa [18] air exhibits good insulation characteristics and has a conduction of typically 10^{-16} to 10^{-17} A/cm^2 [1]. This current is the resultant of radioactive particles and cosmic radiation that permeates into the Earth's atmosphere. When the electric field around any HV apparatus is sufficiently high, energy from the electric field is imparted to free electrons or charged particles. These charged particles are thus excited, begin to collide with one another and if the energy involved is high enough, it may lead to ionisation. The ionisation process is complex [25] and is determined by the mean free path between molecular collisions, whether the collisions are elastic or inelastic, if the density of electrons is optimal, and if the rate of electron production is higher than attachment, etc.

2.3.2.1 Corona Discharge in Air

Observation of corona activity is the first visual indicator of the initiation of the electrical breakdown of air. The electric field needs to exceed a critical threshold (i.e. the corona inception gradient) if moving electrons are to acquire sufficient energy to cause ionisations and hence corona discharges. When electrons from excited atoms return to the natural valence bands, the excess energy is released in the form of photons. This is observed as a bluish (or purple) glow in the vicinity of the high electric field. Corona is thus a partial electrical breakdown of the air – i.e. not sufficient to cause a full arc or flash-over. The different modes of negative dc corona are described as [19]:

- Trichel Streamer;
- Negative Glow;
- Negative Streamer.

While, positive dc corona modes include:

- Burst Corona;
- Onset Streamer;
- Positive Glow; and
- Breakdown Streamer.

The physical manifestation of corona is heavily dependent on the following factors:

- The electrode geometry;
- The air pressure;
- The magnitude and distribution of electric field near the highly stressed electrode; and
- The composition of the gaseous medium between the electrodes.

The fields associated with causing emission currents of a few microamperes is approximately 10^7 to 10^8 V/cm [1]. The discharge process occurs through the following stages namely cumulative ionisation, electron avalanches, secondary ionisation and eventually complete breakdown of the air gap.

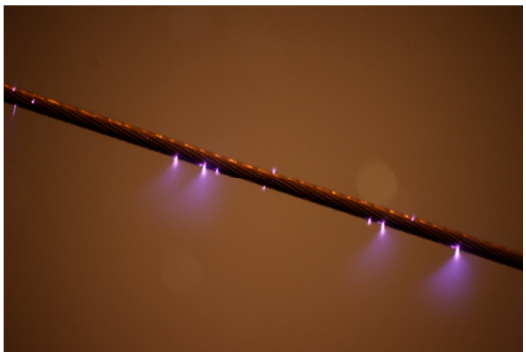


Figure 5: Glow corona from a conductor (ac voltage)

2.3.2.2 Streamer and Leader Mechanism for the Breakdown of Air

Townsend described the ionisation process by conducting experiments to measure the electrical currents involved in the breakdown of air gaps [25]. The work resulted in the Townsend's criteria for electrical breakdown, however, it explained the phenomena of breakdown only at low pressures, corresponding to values of approximately 1000 torr-cm and below.

According to Townsend's theory, electron current growth (i.e. the average current in the air gap) occurs due to ionisation processes only. It is known that breakdown processes also depend on the air pressure as well as the electrode geometry. Secondly, Townsend's theory suggested that time lags in the order of 10^{-5} s between the application of voltage and the actual breakdown itself [28]. Observations were shown that in practice, the breakdown occurs at much shorter intervals of 10^{-8} s. Townsend's mechanism also predicted a diffused form of electrical discharge but in practice the discharges were found to be filamentary and irregular. Streamer breakdown theory was thereafter suggested in order to address these phenomena that was not addressed by Townsend's theory [28].

The streamer theory predicts the development of a breakdown event from a single electron avalanche in which the space charge develop by the avalanche itself is said to transform the avalanche into a plasma steamer. As described in Figure 6, the single electron excited from the cathode side is capable of developing the avalanche across the air gap.

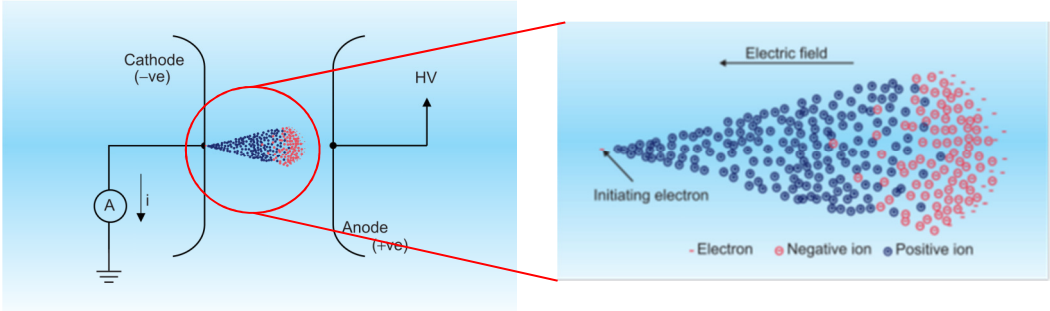


Figure 6: Electron avalanche process (Drawing courtesy of Eskom Power Series [15])

The smaller electrons move at speeds faster than the larger positive ions and by the time the electrons reach the anode the positive ions are not far from their original positions. This charge separation results in the formation of a positive space charge near the anode. The space charge causes an enhancement of the electric field, and secondary avalanches are formed from a few electrons produced due to the photo-ionization in the space charge region. This occurs, at first, near the anode where the space charge is maximum; and results in a further increase in the space charge. This process is very fast and the positive space charge extends to the cathode very rapidly resulting in the formation of a streamer. As soon as the streamer tip approaches the cathode the field is further perturbed and a stream of electrons rush from the cathode to neutralize the positive space charge in the streamer; the result is a spark and the spark breakdown (i.e. flashover) occurs.

Streamer propagation generally occurs in uniform field. For a streamer breakdown process, the electric field has to be suitably high throughout the air gap. The electric field therefore has to supply the energy to drive the ionisation process between the electrodes. The breakdown is characterised by repetitive electron avalanches where the arc generally follows the path of the electric field lines.

A simple quantitative criterion to estimate the electric field E_r which is produced by the space charge, at the radius *r* and that transforms an avalanche into streamer is given by (Meek's theory):

$$E_r = 5.27 \times 10^{-7} \times \left(\frac{\propto e^{\propto x}}{\sqrt{\frac{x}{P}}} \right) \frac{V}{cm} \quad \text{.....(Eqn. 1)}$$

Where:

α = Townsend's first ionization coefficient,

P = Gas pressure in torr, and

x = Distance to which the streamer has extended in the gap.

Now, when $E_r = E$ and $x = d$, Equation 1 is simplified to;

$$\propto d + \ln\left(\frac{\propto}{p}\right) = 14.5 + \ln\frac{E}{p} + 0.5\ln\frac{d}{p} \quad \text{.....(Eqn. 2)}$$

Equation 2 is solved between $\frac{\propto}{p}$ and $\frac{E}{p}$ for which a given p and d satisfy the equation. The breakdown voltage is given by the corresponding product Ed . It is generally assumed that for pd values below 1000 torr.cm and gas pressures varying from 0.01 to 300 torr, the Townsend mechanism operates, while at higher pressures and pd values, the streamer mechanism plays the dominant role in explaining the breakdown phenomena. Through experimentation, the dielectric strength of air for long gaps at STP is 24 kV/cm while a value of 30 kV/cm is reported for short gaps (i.e. 1 cm).

As the air gap becomes larger, the electric field magnitude between electrodes tapers to low levels and consequently the probability of streamer propagation becomes low. For large air gaps greater than 1 m, leader breakdown mechanism becomes more probable. During the leader process, a streamer process is firstly initiated at either the surface of the high voltage electrode (for a negatively charged electrode case) or a short distance away from the surface (for the positively charged electrode case). When the avalanche reaches a critical length with a sufficiently large number of free electrons, the corresponding space charge at the streamer front becomes sufficiently large enough to enhance the local field and to subsequently initiate self-sustained ancillary avalanche processes, until the full gap is traversed and complete breakdown occurs. Due to the fact that the avalanche process is directed by the self-sustained local electric field at the tip of the leader, the arc path may be tortuous or follow the direction of the general field lines. This process is markedly different for different voltages (i.e. ac, transient such as switching or lightning, positive dc and negative dc). This scope of this research project only considered the positive and negative dc cases.

3. Hypothesis and Key Research Questions

Floating objects (whether metallic or not) that are positioned within a dc electric field will affect the average field distribution. The perturbation of the electric field may affect the characteristics of the electrically stressed air gap. If the floating object represents a live worker's approach to the HVDC transmission line/conductor bundle or to any of the hardware attachments on the line, as shown in Figure 7, its presence is likely to intensify the electric field and increase the risk of flashover.



Figure 7: 'Floating' live line worker being lowered onto the Cahora Bassa transmission line by a helicopter

It is reported that under switching impulse voltage test conditions there is a marked decrease in the flashover-voltage when the floating object is positioned towards the centre of the air gap [3]. Under steady state dc conditions the electrical charging of the floating object and space charge effect on the fields may result in a different trend.

The research questions that this investigation aims to address are:

- What is the electrical breakdown characteristic of large air gaps (i.e. larger than 1 m) under steady state HVDC conditions (between 500 kV & 800 kV)?
- Is the breakdown dominated by leader or streamer mechanisms?
- Does space charge have an effect on the breakdown mechanism under HVDC conditions?

- What is the empirical equation for the electrical breakdown of air gaps for a practical working geometries?
- Is it possible to get a repeatable breakdown voltage for large air gaps? (i.e. what is the standard deviation?)
- Is it possible to compare breakdown voltage data with other published data?

Figure 8 shows further examples of live work applications representing a live worker as a floating object in an air gap.



(a) (b)

Figure 8: (a) and (b) Examples of live workers being lowered onto ac transmission lines

4. Research Methodology

In order to investigate the hypothesis, two types of tests were conducted, namely a simple point-to-plane air gap and a point-to-plane gap with the sphere placed at various positions in the gap. The first test intended to be the reference case and was designed to determine the electrical insulation properties of the particular air gap being tested. Both positive and negative polarities were tested for both cases. The voltage source was always applied to the point electrode and the plane was always bonded to earth. The supply voltage was slowly raised at a rate of approximately 2 kV per second. For each test the ambient temperature, relative humidity and barometric pressure was measured and recorded. A corona camera was used to view the ultraviolet (uv) corona discharges around the test objects and a video camera was used to record the test results.

4.1 Simple Rod-to-Plane Breakdown tests

The flashover-voltage of a point-to-plane air gap (i.e. without the sphere) was determined for reference purposes. The total gap size was determined by the maximum voltage that could be practically flashed-over using the power supply. After the total gap size was determined, positive dc voltage was applied to the point electrode and the voltage was raised until a flash-over occurred. The flashover tests was repeated between three and ten times at each position to determine the repeatability thereof. A time of one minute was allowed between each test in order for the static and space charge to dissipate.

4.2 Floating Metallic Sphere Breakdown Tests

The second series of tests involves inserting a sphere into the air gap between the point electrode and the plane. The sphere was initially located closer to the rod and the flashover tests were repeated. The position of the sphere was then systematically adjusted until it approached the ground plane. After a series of tests, the total gap size was reduced and the procedure was repeated. The total gap distances tested were 1 m, 1.25 m and 1.4 m. The sphere was electrically discharged to ground after each test.

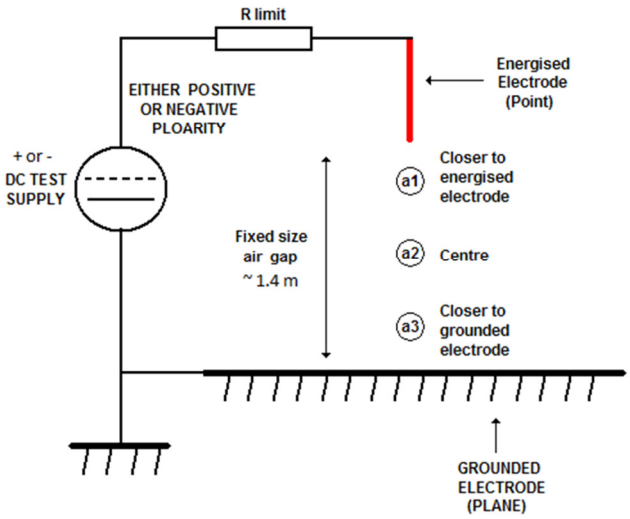


Figure 9: Schematic representation of the test setup

The sphere was positioned in various places within the gap (as indicated from a1 to a3 in Figure 9). The negative polarity case was also tested. For the purpose of this research three gaps were defined. These are:

- The 'total gap' size which relates to the distance between the tip of the point electrode and the ground plane.
- The 'primary gap' which is the distance between the tip of the point electrode and the top of the floating sphere.
- The 'secondary gap' which is the distance between the tip of the metallic protrusion (at the bottom of the sphere - see section 5.3) and the ground plane.

4.3 Test program

The summary of the test program is as follows:

Point-to-plane tests:

- Positive polarity 1m and 1.25 m gaps
- Negative polarity 1m and 1.25 m gaps

Floating object tests:

- Positive polarity: 1m, 1.25 m and 1.4 m gaps with floating objects at various locations within each gap.

- Negative polarity: 1m gaps with floating objects at various locations within each gap.

4.4 Correction for Standard Temperature and Pressure

The test were conducted in accordance with the IEC60060-1 standard [18], and corrected (as per the standard) for Standard Temperature and Pressure (STP) as well as for humidity. It must be noted that the tests were conducted outdoors. The location of the laboratory was Sunninghill, Johannesburg at an altitude of 1550 m above sea level.

5. Experimental setup

In order to conduct the tests, a power supply and test object had to be developed. Figure 10 shows the electrical equivalent circuit for the test.

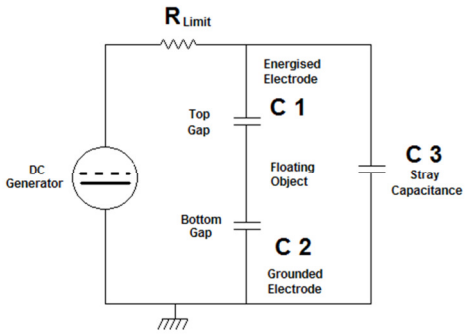


Figure 10: Equivalent circuit of the test setup

5.1 High Voltage – Direct Current Power Supply

The research intended to test air gaps larger than 1 m. In order to break down air gaps of this size, a high voltage is required. The dielectric strength of air is approximately 26.6 kV/cm (at sea level)[1].

In order to conduct the tests an adequately rated power supply was required. Because of the high voltages required for this test, Eskom's Corona Cage test facility was used. The

facility did however have a limitation of only a 400 kV ac (phase to ground) transformer. This limited the maximum gap size that could be tested.

The dc power supply used for this work consisted of an arrangement of six high voltage diodes forming a single phase, half wave rectifier. Ripple capacitance was implemented using an existing a parallel combination of 50 pF standard capacitor and 2000 pF coupling capacitor.

5.1.1 Design of the Rectifier

The power supply consists of a 500 kV (phase to ground) transformer with a nominal current rating of 20 mA and a surge current of 1 A. The rating of each diode was 250 kV with a maximum current of 500 mA each. The diodes were arranged in a bank with three in series and two in parallel. The series arrangement provided the voltage rating of 750 kV while the parallel bank allowed for a higher maximum current of 1 A.

The tests were conducted outdoors. The individual diodes were encased in a fibreglass housing (Figure 11 (a)) and had a connecting length of 1 m.



(a) (b)

Figure 11: (a) Uncovered original diode stack, (b) Diode covered with silicone rubber sheaths

There was a concern that the electrical creepage of the diode stack was insufficient for an outdoor installation. From a safety viewpoint, the individual diodes were thus covered with composite insulator sheds (Figure 11 (b)), to provide a higher creepage to limit the

possibility of tracking across the surface of the fibreglass. The diode stack was attached to a live-line pole for mechanical strength (Figure 12) and electric field grading rings were installed around the diode attachment points to manage the expected high fields in that area (Figure 13).



Figure 12: Rectifier mounting platform



Figure 13: Hardware rings used around connection points

No specific technical design was done for the dimensioning of the grading rings, rather the implementation was based on the fact that these rings were available at the time of the construction. The diode arrangement was installed in the HV circuit as indicated in Figure 14.



Figure 14: Installation of the diode arrangement in the HV power supply circuit

The ac transformer had a maximum current capability of 20 mA. During flashover, the current could temporarily surge to magnitudes higher than the rating of the transformer, which was rated at 1 A. As an additional precaution to protect the transformer, a series connected current limiting resistor was used. Due to the magnitude of the high voltage (and energy), a water resistor was selected for this application (Figure 15) as it was available at the time of the test. The resistor was constructed using PVC tube with the end sealed with end caps. The end caps were modified to hold the electrical connection points. The resistor was filled with deionised water. The total resistance of the water resistor was measured to be 12 MΩ. In accordance with Ohm's law, during a flashover event, at 600 kV, the water resistor will limit the surge current to approximately 50 mA, which is within the safe operating limits of the transformer and diodes.



Figure 15: Water resistor and voltage divider

A 200 kV resistive voltage divider was used to measure the supply voltage. The divider used had a measurement ratio of 2000:1. The divider had a resistance of 200 MΩ. Due to the limitation of the maximum voltage limit of the divider, the power supply voltage of only up to 200 kV was verified. Further information relating to the power supply voltage and ripple is presented in Section 5.1.3.

The supply current was measured on the ac side of the rectifier, using a clamp-on current transformer (CT) connected to a multimeter. The multimeter was installed on the secondary (HV) side of the ac transformer and as such would be at full voltage potential (Figure 16). A conventional multimeter would be ineffective as it would be difficult to read the screen due to the location thereof. An infrared connected removable display type multimeter was used and the screen was located at ground level where it was convenient to monitor the supply current.



Figure 16: Removable display multimeter connected to the ac side of the rectifier

5.1.2 Initial Commissioning Tests

Careful considerations to safety needed to be taken into account when testing and commissioning the power supply. The first tests included energisation at a low voltage of 80 kV (i.e. the switch-on voltage of the ac transformer). The inrush current was monitored and was determined to be at a safe magnitude.

In order to determine the effectiveness of the grading rings for managing the electric fields around the diodes, an inspection was done using a corona camera. The camera displayed UV discharges in the areas of high fields (Figure 17). The discharge events are indicated by the white dots overlaid on the image. These corona discharges are undesirable and could lead to spurious flashovers occurring across the diodes. This would be unsafe. Initial

images indicated some discharge activity and minor modifications were made to plastic cable ties and connecting wire to eliminate the discharge activity.

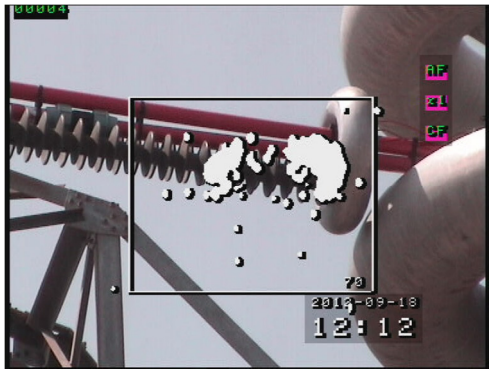


Figure 17: CoroCAM® image showing corona discharges on the rectifier

The second series of tests involved slowly increasing the ac voltage while carefully monitoring the supply current, corona on the rectifier and the temperature of the water resistor. After a series of tests it was determined that the power supply was safe to operate. This arrangement allowed a usable voltage of up to +640 kV dc.

5.1.3 Voltage Ripple

Using the resistive voltage divider, the voltage and ripple of the system was verified up to 200 kV. For voltages greater than 200 kV, it was assumed that the dc voltage was equal to the peak root mean square (rms) voltage and that the ripple was within a 5 % tolerance. At 140 kV DC the ripple is less than 2% (Figure 18) and at 200 kV the ripple was only 2.3%. Since the circuit was not loaded (i.e. open circuit) it can be assumed that there is linearity in the ripple at the higher voltages.

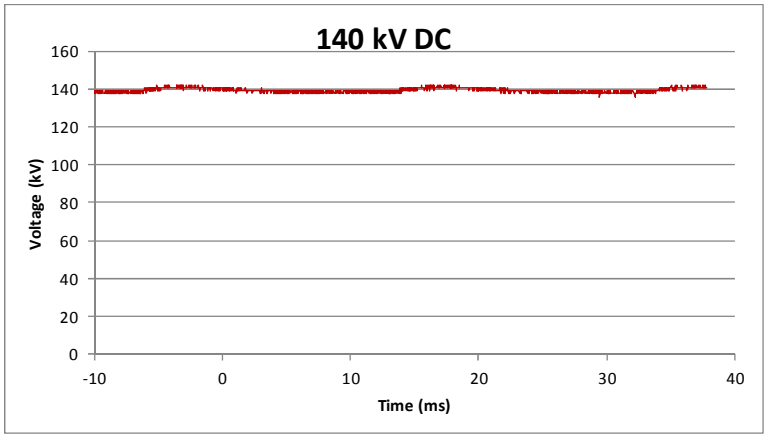


Figure 18: Graph showing measured dc voltage

Figure 19, shows the measurement of the ripple on the rectified supply. The ripple has a peak magnitude of approximately 2.5 kV (1.7 % of the rectified voltage). The offset in the graph is due to the measurement setup. The level of ripple is considered adequate as it is less than 5 % [18].

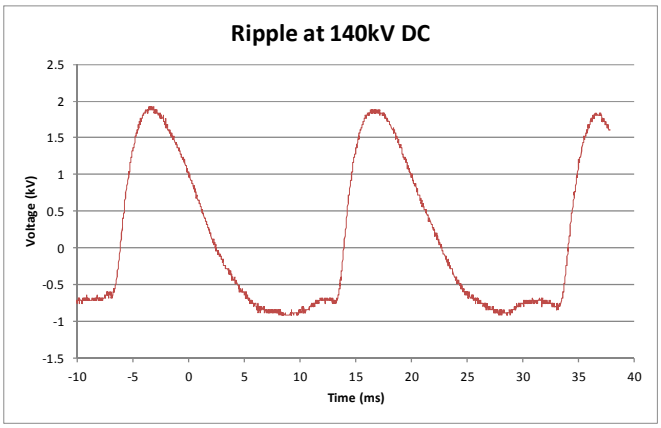


Figure 19: Graph showing the ripple measured on the power supply

5.2 Simple Point-to-Plane Test Setup

The point to plane setup was constructed using copper tubes and a wire mesh. The point was a 20 mm diameter copper tube. The tube end was sealed with a copper end cap. The length of the tube was 1.5 m. The plane was constructed using a mild steel wire mesh which was placed directly on the concrete floor. The wire mesh was electrically bonded to the earth mat of the test facility. Figure 20, indicates the respective components of the circuit.

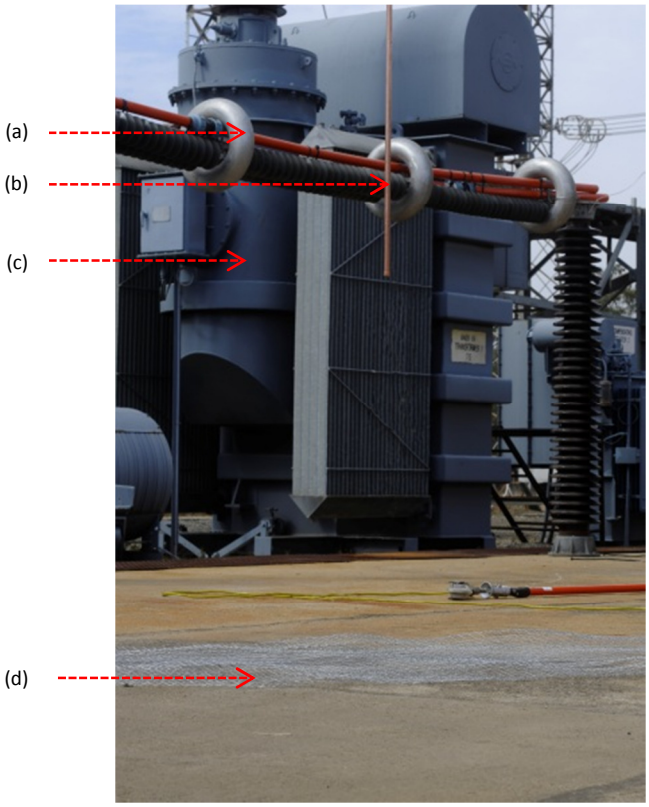


Figure 20: Test setup for the rod-plane experiment

(a) Rectifier diode stack (pictured in the background)
(b) Point electrode (pictured in the foreground)
(c) 400 kV ac supply transformer
(d) Ground plane

5.3 Particulars of the Metallic Sphere

The sphere was a 300 mm diameter aluminium ball. A 30 mm protrusion was implemented on the bottom of the sphere to replicate practical situations where it is difficult to maintain smooth surfaces. The presence of the protrusion results in a lower breakdown and may

suppress the accumulation of free charge on the sphere [3]. The sphere was hollow and air-filled. Figure 21, shows the test setup for the floating metallic sphere tests, while Figure 22 presents a close-up view of the sphere itself.



Figure 21: Test setup for the floating sphere experiment

(a) Water resistor
(b) Point electrode
(c) Floating sphere
(d) Porcelain stand-off insulators
(e) Ground plane
(f) Primary gap
(g) Secondary gap

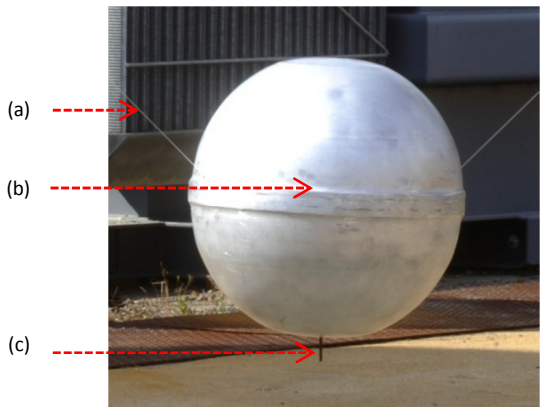


Figure 22: The sphere used in the tests, showing the 30 mm protrusion

(a) Nylon string
(b) Aluminium sphere
(c) 30 mm protrusion at the bottom of the sphere

The sphere had a raised section around its centre. The raised area was due to the method used in the construction of the sphere (see Figure 22).

5.4 Air Gap Dimensions for the Floating Sphere Tests

The floating sphere setup was the same as the simple rod to plane setup, with the addition of the floating sphere suspended in-between the rod and plane. The metallic sphere was suspended between two, 2 m tall substation post insulators, using nylon string. The total air gap distance was varied between 0.75 m to 1.4 m.

6. Test Results

This section presents the results that were obtained from the tests. The point-to-plane test results are used as the reference case and is also compared with other test data.

6.1 Results of the Point-to-Plane Tests

Tests were done for both positive and negative polarity. The results are presented below.

6.1.1 Positive Polarity Results

Two gap distances were tested. The results are the average of at least ten flashovers per gap length. Table 1, below, presents the results corrected for STP as per [18]:

Table 1: Results of the positive polarity point to plane tests

POSITIVE POLARITY	AVERAGE FLASHOVER-VOLTAGE (kV)	MINIMUM FLASHOVER-VOLTAGE (kV)
1.00 m air gap	484	476
1.25 m air gap	640	635

It was not possible to flashover the 1.4 m air gap using the available power supply. When plotted together with data from previous gap testing [20, 21], as shown in Figure 23, a linear trend is obtained for the range of rod to plane gaps tested. The coefficient of determination (R^2) is close to a value of one (1), indicating a good agreement between the linear regression curve (shown in black) and the data. In Figure 23, the data up to 750 mm are from previous tests [20].

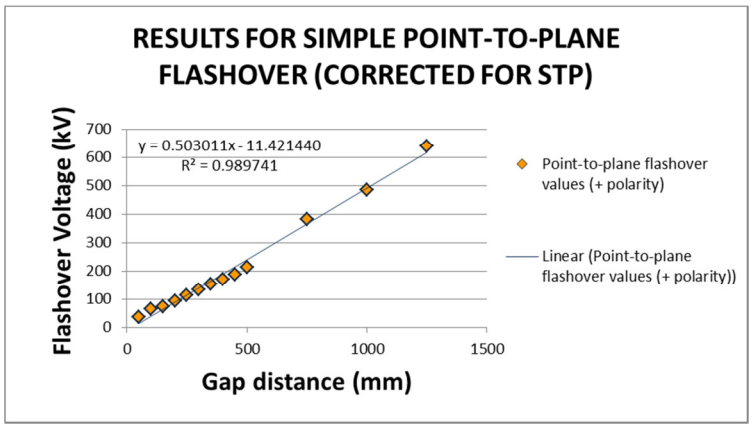
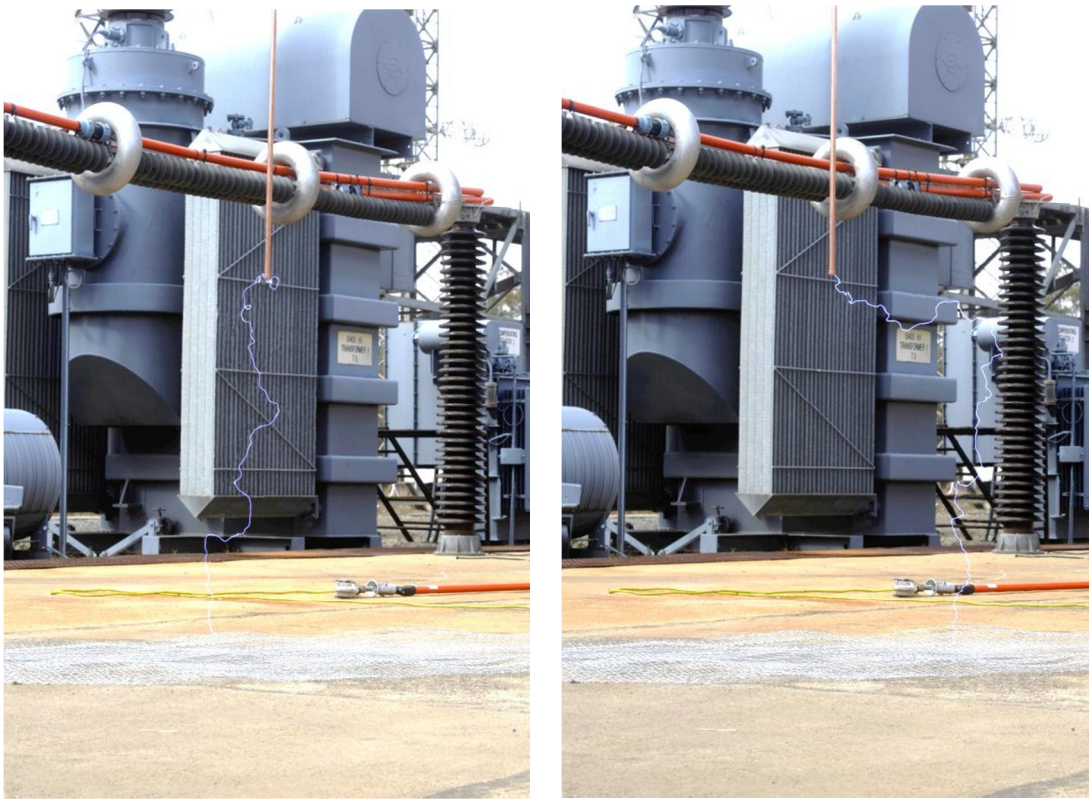


Figure 23: Graph showing linearity for positive polarity dc flashover tests

The results indicate that this particular setup had an electrical insulation strength (under positive polarity) of approximately 484 kV/m. Figure 24 show pictures of the flashover.



(a) (b)

Figure 24: (a) and (b) Pictures showing arc behaviour for the positive polarity point to plane tests

In many cases, the arc did not follow a straight, shortest or direct path between the electrodes. Figures 24, 25 and 36, respectively, show the elaborate arc path within the gap.

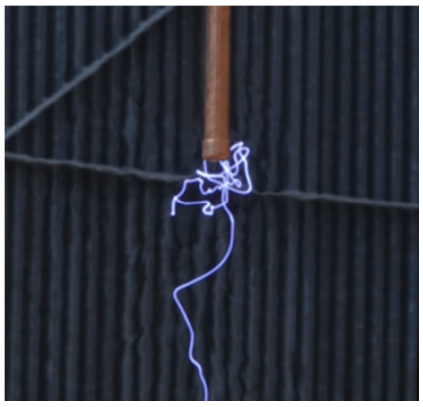


Figure 25: Picture showing tortuous arc path at the positive electrode.

Figure 25 was recorded with a digital camera having a shutter speed of 0.12 ms. The image is therefore a pseudo-steady state representation of the discharge during the flashover.



Figure 26: Picture showing arc initiation a short distance away from the tip of the point electrode

6.1.2 Negative Polarity Results

Negative polarity dc generally requires a higher voltage level to flashover the same size air gap than positive dc [1, 20, and 21]. The limitations of the power supply voltage only allowed for the safe testing of a 0.42 m air gap. Table 2 shows the results of the negative polarity point to plane tests. Detailed test results are listed in Appendix A.

Table 2: Results of the negative polarity point to plane tests

NEGATIVE POLARITY	AVERAGE FLASHOVER-VOLTAGE (kV)	MINIMUM FLASHOVER-VOLTAGE (kV)
0.42 m air gap	408	382
1 m air gap	-	-
1.25 m air gap	-	-

When plotted together with data from previous gap testing [20], shown in Figure 27, a relatively linear trend was observed for the range of rod to plane gaps tested.

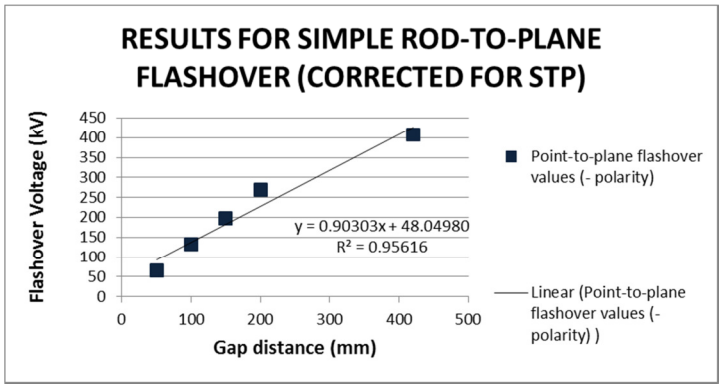
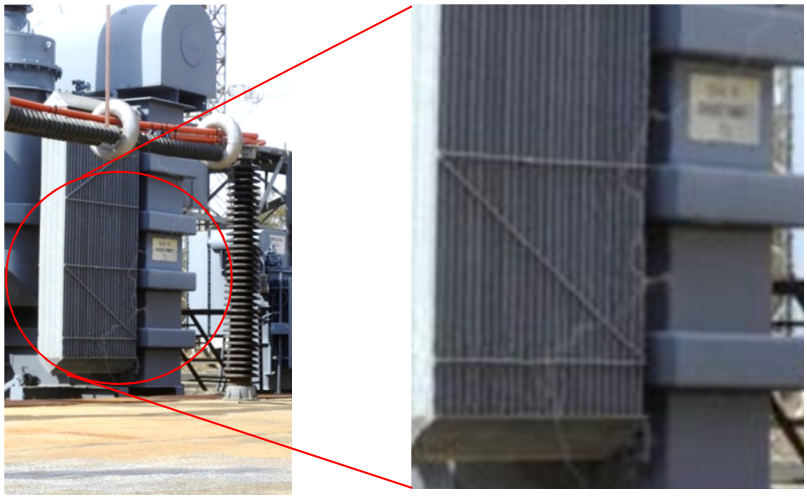


Figure 27: Graph showing linearity for positive negative dc flashover tests

The results indicate that this particular setup had an electrical insulation strength (under negative polarity) of approximately 951 kV/m. This is significantly higher than the positive polarity case. This result is as expected and is attributed to the specific physics relating to the development of the electron avalanche around the negatively stressed electrode [15]. Unlike the positive polarity case, the relatively light electrons are quickly accelerated away from the electrode and the relatively heavy positive charges are slowly drawn towards to the electrode. The migration of the electrons away from the tip may serve to decrease the effective surface gradient on the surface of the point as well as the average electric field in the immediate vicinity of the point electrode. The electrons are propagated in a decreasing field; hence, a higher voltage is required for a complete flashover to occur.

There were several differences noted for the negative polarity case when compared to the positive case. For the negative case, the steady voltage was held for a longer period (approximately a minute longer) than the positive case, before a flashover occurred. As shown in Figure 28, at the maximum voltage, discharge/plasma channels were evident, prior to flashover occurring. In other words, the channels were visible without any arc having occurred at that point.



(a) (b)

Figure 28 (a) and (b): Faint plasma channels observed during the negative polarity tests

6.2 Repeatability of the Breakdown Voltage versus the Gap Size

For the 1 m positive polarity case, the standard deviation was calculated to be 6.8 kV, which is a 1.3 % variation in flash-over voltage.

For the 1.25 m positive polarity case, the standard deviation was calculated to be 4.5 kV, which is a 0.7 % variation in flashover voltage.

For the 0.42 m negative polarity case, the standard deviation was calculated to be 4.5 kV, which is a 9 % variation in flashover voltage

The flash over-voltage for the positive polarity case is within a tolerance of 5 % of one another. The tests are deemed to be repeatable.

The standard deviation for the negative polarity case is significantly higher than the positive case. The negative polarity flashover voltage is seen to be less repeatable than the positive case.

6.3 Results of the Floating Sphere Tests

Detailed test results are shown in Appendix B and C, respectively.

6.3.1 Positive Polarity Case

Figure 29, shows the actual results obtained for the positive polarity case, while Figure 30 shows the results corrected for STP. The graphs are a plot of the flashover-voltage against the primary gap size (viz. the plots show the recorded flashover-voltage as the sphere was moved from a position closer to the point electrode to a position closer to the ground plane). As the total gap length was increased, more test positions were available for the positioning of the sphere; therefore, there are more data points in the respective curves. The flashover-voltage presented is the lowest recorded value for that series of consecutive tests, at a specific gap length, and not the average value. The lowest value is representative of the worst case.

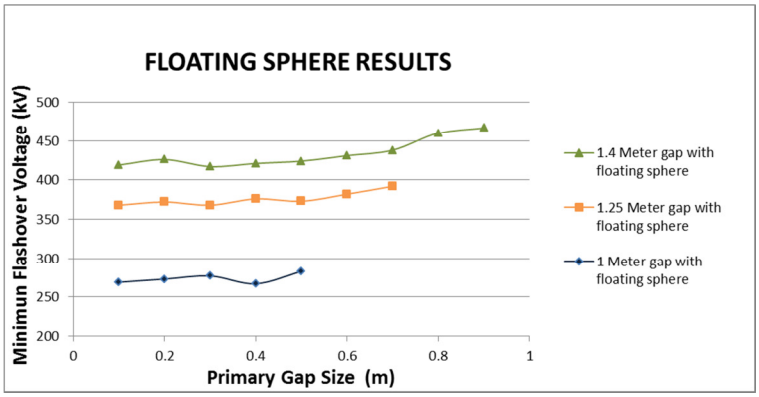


Figure 29: Graph showing the results obtained for the positive polarity between gap sizes ranging from 1 m to 1.4 m (uncorrected data)

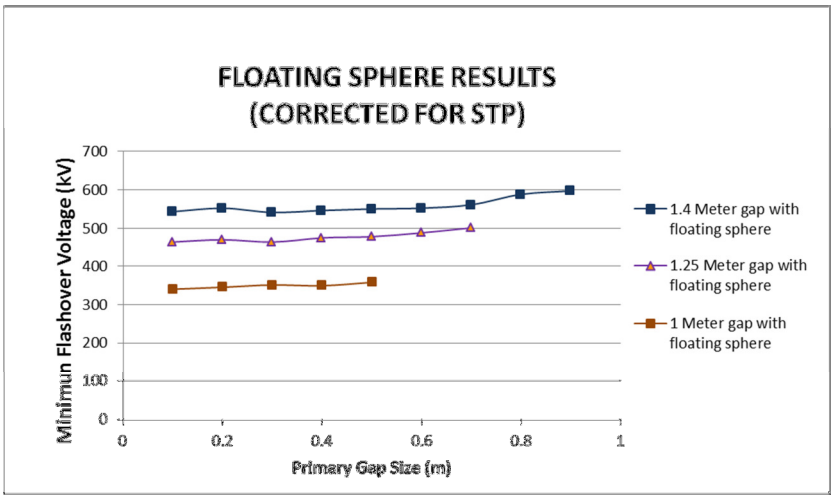


Figure 30: Graph showing the results obtained for the positive polarity floating object tests (data corrected for STP)

For the smaller primary gap size the position of the sphere did not significantly impact the flashover-voltage. It was observed that the flashover voltage had a tendency to increase as the primary gap became larger. For the 1.4 m total gap case, there was a deviation of 10 % from the smallest primary gap to the largest. A 6 % deviation was calculated for the 1.25 m total gap case and only 5.6 % for the 1 m case.

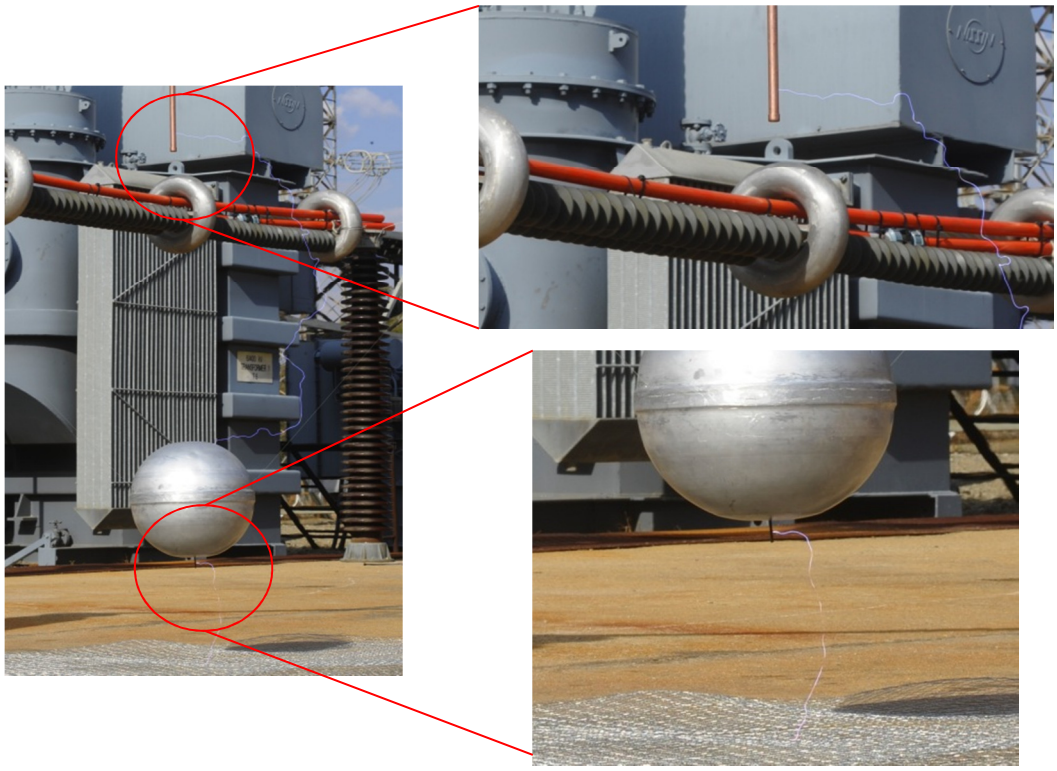


Figure 31: Arc attachments for the positive polarity floating object tests, where the sphere was positioned in a location closest to the ground plane

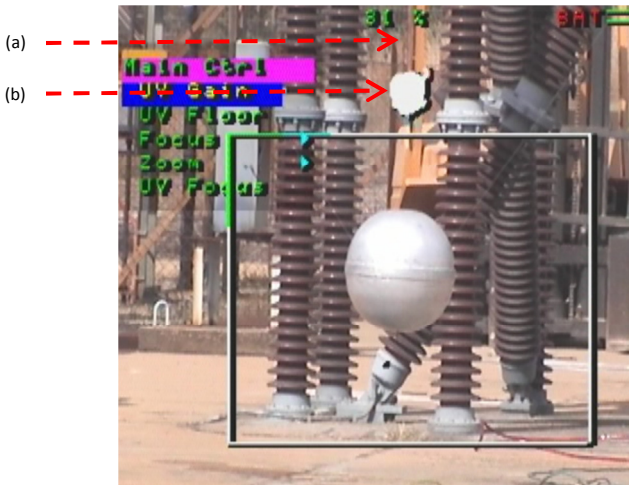


Figure 32: CoroCAM® image showing sustained corona discharge at the point electrode.

(a) Copper point electrode.

(b) Corona camera rendering of the constant discharge activity occurring at the electrode.

Figure 31 shows an event where the arc did not originate at the tip of the electrode, but rather along its length (for the positive polarity case). On review of the CoroCam® image, (Figure 32), it is seen that there is a steady continuous electrical discharge around the tip of the rod electrode. This is visible as a cluster of white dots in the region of uv discharge activity. From the observations shown in Figures 31 and 32, it is proposed that this type of discharge activity results in a build-up of space charge of similar polarity as that of the energised rod – in this case, positive pockets of charge. The area of positive charge around the positively energised electrode may have an effect of lowering the surface gradient around the tip of the conductor. In the case of the positively energised electrode, the arc process is initiated a short distance away (possibly a distance of a few millimetres) from the electrode. In this area, the field is sufficiently large to initiate discharge activity. The electron movement occurs in an increasing field (i.e. towards the energised electrode). It is postulated that as this streamer propagates towards the electrode it follows the electric field lines. As described above the field is lowered by the space charge around the tip of the electrode. The streamer discharge therefore attaches to the electrode at the point where the field magnitude is the largest (i.e. a short distance away from the tip). On attachment of the streamer to the electrode, a plasma channel is established. Some of the charge from the electrode is transferred to the tip of this new plasma channel. The streamer process then repeats in the direction of the electrode with the overall effect of streamer tip moving downward towards either the floating object or the ground plane.

6.3.2 Comparison with the Reference Case

From Figures 33 and 34, it can be seen that there is a noted reduction in the insulation strength of the air gap, with the floating sphere present.

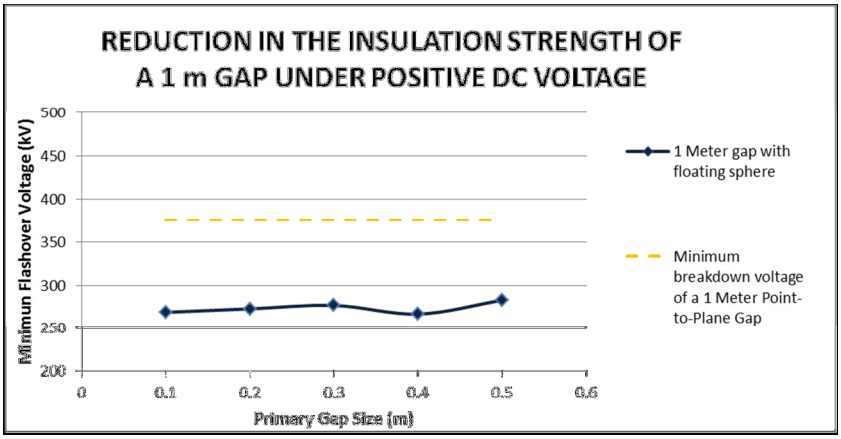


Figure 33: Graph indicating the reduction in insulation strength for the 1 m gap

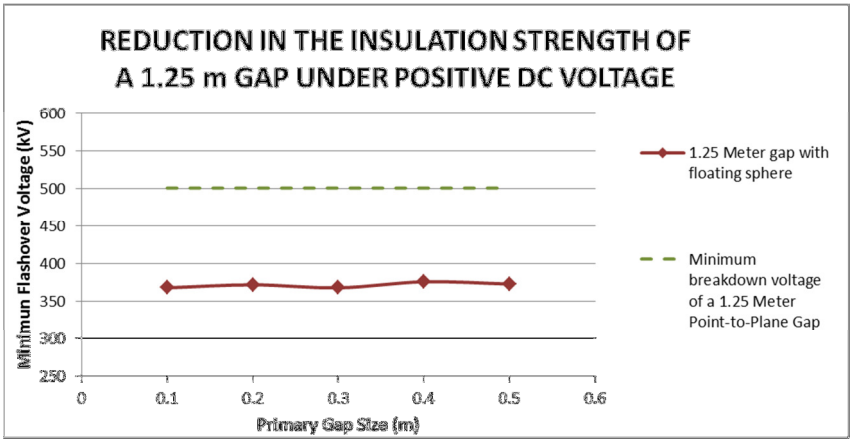


Figure 34: Graph indicating the reduction in insulation strength for the 1.25 m gap

For the 1 m total gap case, there is a reduction of approximately 71% (Figure 33), while a 73% reduction was calculated for the 1.4 m gap (positive polarity case)(Figure 34).

6.3.3 Further Images for the Positive Polarity Case

It was observed that the arc also did not necessarily follow the direct or shortest path between the electrodes. A tortuous arc path was observed as shown in Figure 35. Also evident is the flame like behaviour of the arc terminating on the protrusion at the bottom of the sphere.



Figure 35: Erratic arc path

In two separate tests, it was observed that the arc ignored the floating object (Figure 36). The sphere was positioned in the centre of the gap. This result was not expected. For a total gap size of 1.4 m, a calculation using the linear equation shown in Figure 23, shows that a voltage of 692 kV would be required to break down the gap. The power supply was not capable of supplying this voltage. Practically, this situation could exist if the floating sphere became statically charged with an opposite polarity of the point electrode.



Figure 36: Image showing the arc evading the sphere

In another test, the image recorded using the CoroCAM ® (Figure 37) shows that the arc did not originate directly on the protrusion at the bottom of the sphere. Rather, the arc initiated a short distance away from it.

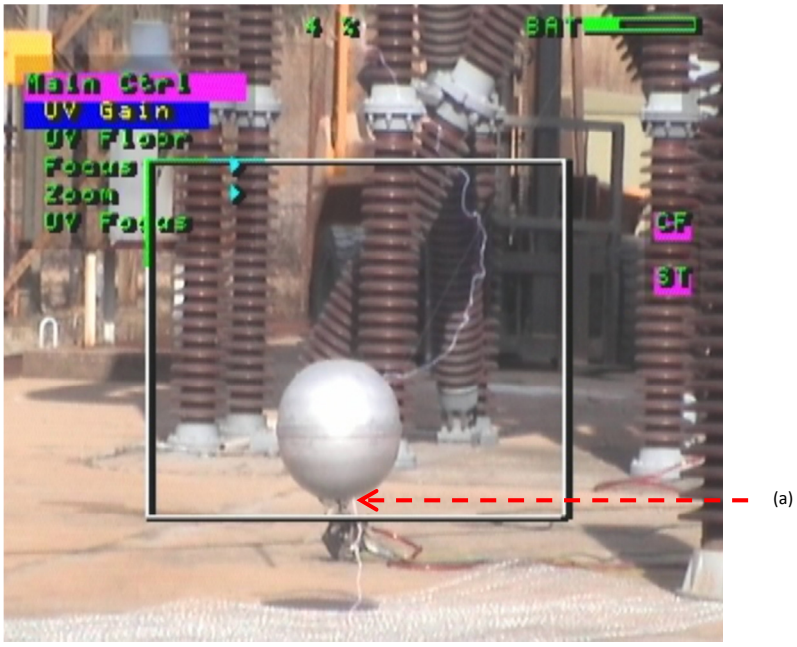


Figure 37: CoroCAM® image showing the arc path ignoring the protrusion at the bottom of the sphere

(a) Arc originating from the sphere and not the protrusion

6.3.4 Negative Polarity Case

Detailed test results are shown in Appendix C. The graphs (Figure 38 Figure 39) shows the results obtained for the negative polarity case. The data plotted is the uncorrected and corrected values, respectively. As explained in section 6.1.2, above, the maximum power supply voltage limited the total gap size that could be tested. By trial and error technique, only the 1 m and 0.75 m total gaps (with a floating objects) were tested.

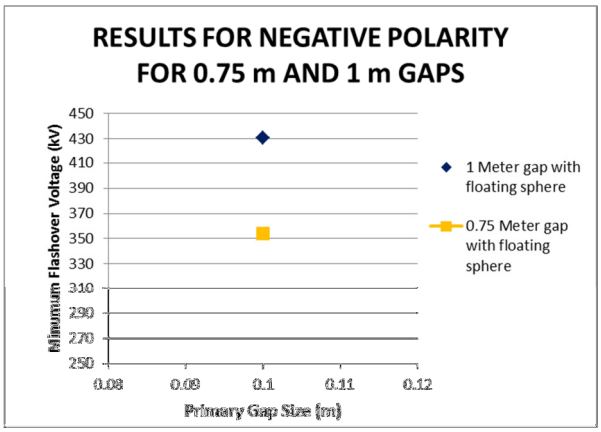


Figure 38: Graph showing results for the negative polarity tests (uncorrected for STP)

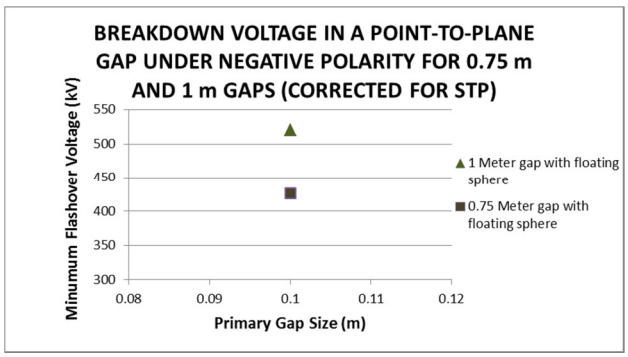


Figure 39: Graph showing results for the negative polarity tests (corrected for STP)

Given that a result for only the 0.42 m point to plane gap was obtained, it is not possible to compare the results to a reference case, as was done with the positive polarity results. This result is intriguing as the presence of a 300 mm diameter sphere allowed for the testing of a 1 m total gap size – i.e. a 680 mm increase in size from the point-to-plane case.

6.3.5 Images for the Negative Polarity Tests

In certain cases it was observed that the arc did not terminate or originate from the tips of the electrodes, but rather along its length. For some tests, the arc was observed to originate from the sides of the sphere and not necessarily from the protrusion itself (Figure 40 and Figure 41).



Figure 40: Picture showing the arc origination at the bottom of the sphere and not the protrusion

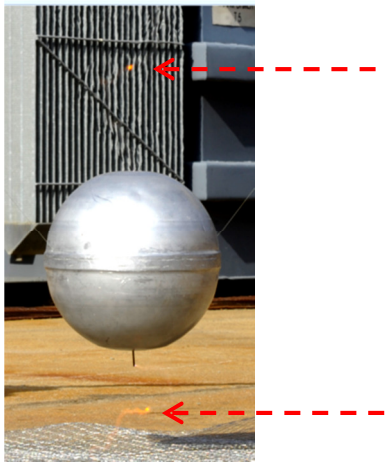
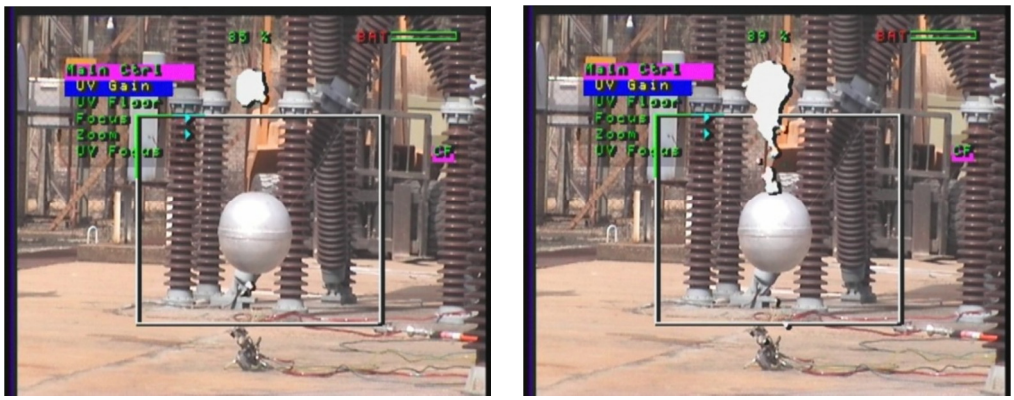


Figure 41: Picture showing spark discharge activity in the air space between the HV point electrode and the sphere (indicated by the red arrows)

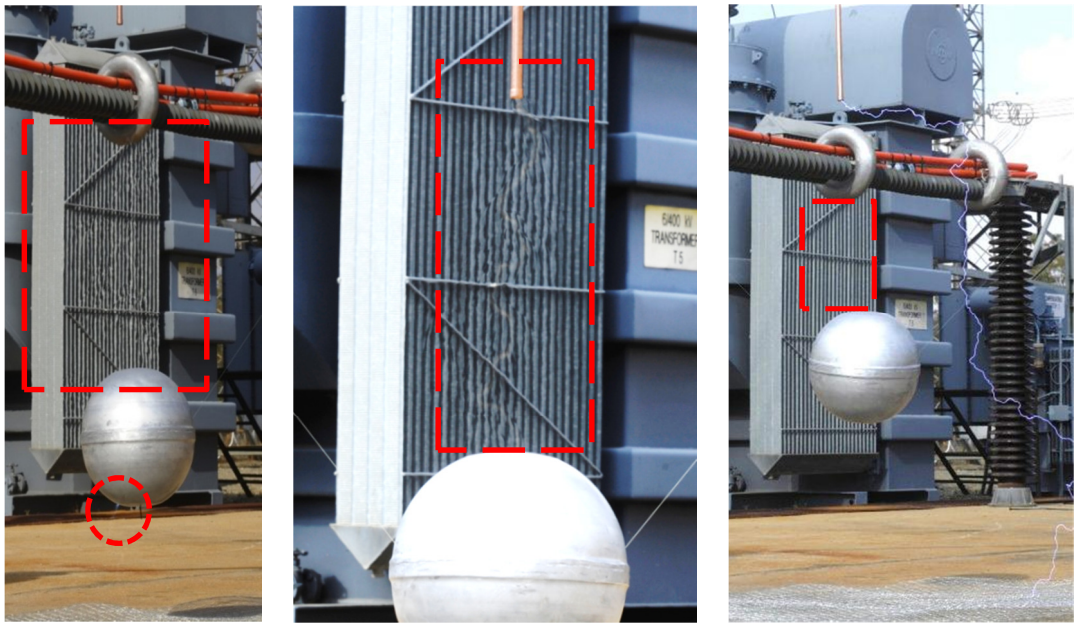
The images obtained from the CoroCAM® (Figure 42) and the photograph above (Figure 41) show that for the negative polarity tests there were sustained discharge activity at the tips of the point electrode and the protrusion. Such corona activity leads to the development of pockets of alternating space charge and may cause an alteration (i.e. decrease) of the space potential around the electrodes. The arc, following the direction of the high electric field lines may therefore diverge away from the areas of low fields (i.e. the areas around the electrodes).



(a) (b)

Figure 42: CoroCAM® images[1] showing (a) sustained discharge activity point and protrusion, and (b) in the air gap between the point and the sphere

In Figure 43, visual corona discharge activity is evident at the bottom of the sphere itself and not on the tip of the protrusion. This discharge was present prior to the flash-over event and is indicative of a extremely high charge on the sphere. It must be noted that for this particular test, the sphere was located in a position closest to the ground plane with a sphere to ground gap distance of 0.35 m. Also visible in the image is the physical electric field stress of the primary air gap, which presents as thermal emissions [1].



(a) (b) (c)

Figure 43: In figures (a) and (b) above, the heat stress is evident as it distorts the reflection of the cooling fins of the supply transformer, which are normally straight, as shown in (c). (a) and (b) are images captured prior to the flashover.

[1] The cluster of white dots is the rendering of the location of the uv discharge activity, as represented by the CoroCAM®

6.4 Repeatability of the breakdown Voltage versus Gap Size

For the positive polarity floating object tests, a total of twenty one combinations were completed. The worst standard deviation recorded was 7.12 kV, which related approximately to a 1.5% variation in the voltage.

For the negative polarity floating object tests only two combinations were completed. The standard deviation for the 1 m total gap - with a primary gap of 0.1 m, was 0 kV while the standard deviation for the 0.75 m total gap - with a primary gap of 0.1 m, was 21.8 kV.

It can be seen that the negative polarity case is considerably less repeatable than the positive case. This result agrees with the results shown in Section 6.1.2.

7. Discussion and Analysis

There are two main physical processes occurring within the air gaps in the test setup. Firstly, the point electrode is charged via the power supply. The tips of the electrode are brought into corona and space charge is created within the air primary air gap.

Secondly, the electric fields established within the test area serve to charge the floating object. The sphere alters the fields in the secondary air gap. The charge on the sphere may become sufficiently high enough such that the tip of the protrusion exceeds the corona inception gradient. Space charge is then generated in the secondary gap. This phenomenon is evident in Figure 42 (a), where both the point electrode and the tip of the protrusion are observed to have steady corona discharge activity and in Figure 42 (b) where discharge activity is evident in the primary air gap. It is noted that this is a steady state scenario.

7.1 Comparison with Published Literature: Research conducted by Rizk

Previous research using floating spheres under switching impulse conditions [3] indicated a distinct decrease in breakdown voltage for the sphere in the quartile of the gap closest to the high voltage electrode (see Figure 44, below). The gaps tested in [3] were larger than that tested during this work and the voltage magnitudes were significantly higher. Further, switching impulses occur much quicker than constant dc and the mechanism of the air breakdown may be different.

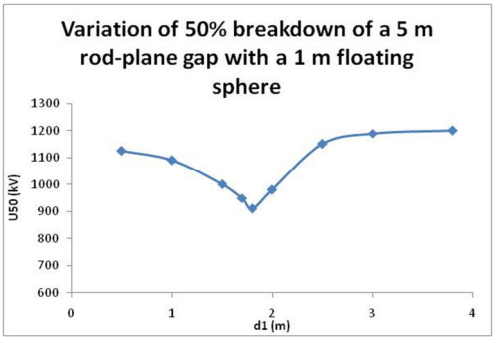


Figure 44: Graph of generalised results from [3]

The research done by Rizk shows that there is a distinct decrease on the flash over-voltage as the floating object moves away from the point electrode, until a critical point (some distance away from the electrode tip in the primary gap) at which where it starts to increase again. The research done by Rizk shows that the electrical strength of the air gap

is strong when the sphere is closest to the point electrode. As the sphere moves away, the gap strength decreases until a critical distance is obtained. As the sphere is moved further away from this critical distance the electrical strength of the air gap then increases. This work indicates that there could be different air break down mechanisms occurring in each gap and that either the primary or secondary gap could break down first.

Unlike the case for switching impulse voltage, the results of this research indicates that there is no critical primary gap size where the flashover-voltage is the lowest. The results obtained seem to indicate that the primary gap breaks down first followed immediately by the secondary gap. As the sphere is moved to positions further away from the energised point electrode, the flashover-voltage increases.

7.2 Limitations of the Power Supply

The maximum voltage of the test supply was approximately 600 kV. This limited the maximum size of air gap that could be achieved. For positive polarity, the maximum size of the air gap that could be safely flashed-over was 1.25 m (point-to-plane setup). For the negative case, the largest gap was 0.75 m. For the same size of air gap, negative polarity requires a higher breakdown voltage than positive polarity. This was evident as illustrated in Figure 45 as well as [20, 21]. The power supply was unable to provide sufficient voltage magnitude to breakdown a larger gap. The test was stopped in order to protect the power supply.

The voltage limitation did not allow for the replication of practical line and tower geometry gap sizes. Due to the scaling of the gap and floating object sizes, the tests therefore cannot be directly related to live working conditions.

7.3 Leader or Streamer Breakdown Mechanism – Discussion based on Test Observations

Erratic arc behaviour was observed for some tests. Such behaviour is normally observed when the breakdown process occurs via the leader mechanism. Similar to lightning strike development processes, the electric field that is independently generated at the tip of the leader has the greatest influence on the path taken by the flash. For the leader process, this path appears random and erratic. Streamer breakdown may also appear erratic if the electric field is sufficiently perturbed by the presence of space charge.

In Figure 36: Image showing the arc evading the spherethe arc is seen to have completely evaded the sphere. If the breakdown was characterised by streamer mechanism, then the arc should have taken the shortest distance to bridge the entire gap (i.e. to terminate on the sphere) [26].

Further, the temperature associated with the leader development process is significantly larger than for the streamer development process. There is little heat energy generated by the streamer propagation process and it does not significantly affect the ambient temperature around the breakdown channel. Due to the greater heat energy involved with the leader breakdown process there is generally an increase in the ambient temperature around the arc channel. Such temperature variation has been observed in Figure 43. Streamer breakdown, being dependant on the background electric field, usually has a linear relationship between the flashover-voltage and the gap size.

7.3.1 Analysis of the Negative Polarity Results

Figure 45 shows the difference in linearity for shorter and longer gaps, respectively. The data plotted in Figure 45 is the same data that has been presented in Figure 27, but with different linear regression curves fitted separately, firstly for the section of gaps up to 200 mm, and secondly between 200 mm and 500 mm. As expected, analysis of the data indicates a linear relationship for small gaps (up to 200 mm). Using the linearity relationship for the section of the smaller gaps, a higher flashover-voltage (i.e. -566 kV) was expected for the 420 mm gap size. This could possibly indicate that the breakdown mechanism changed from streamer to leader breakdown past the 200 mm length point; however, this result on its own merit is inconclusive.

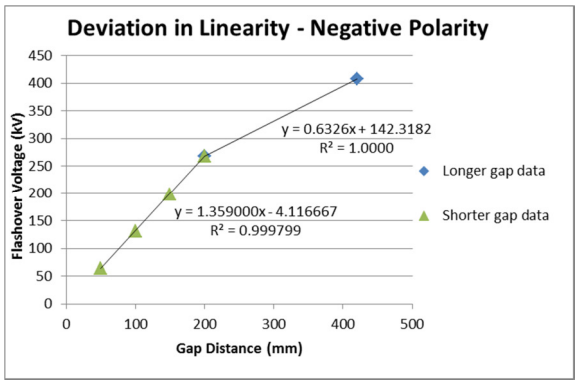


Figure 45: Graph indicating the change in linearity between shorter and longer gaps (Negative Polarity case). Data corrected for STP.

7.3.2 Analysis of the Positive Polarity Results

Figure 46 has also been analysed in a manner similar to Figure 45, as described in the preceding section. As expected, Figure 46, also shows linearity for the shorter and longer gaps, as plotted separately. It is evident that the gradients of the data points are different (viz. 0.51 for the longer gaps and 0.38 for the shorter gaps); however, it is not as large as the negative polarity case. No conclusive conclusion can be drawn from this analysis.

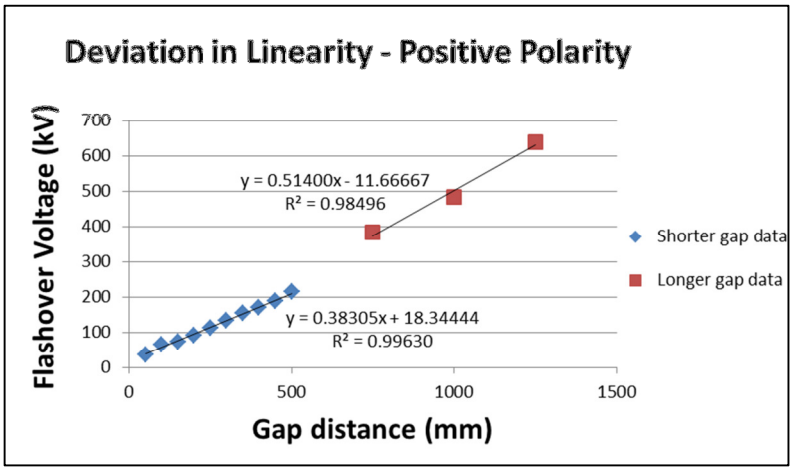


Figure 46: Graph indicating the change in linearity between shorter and longer gaps (positive polarity case). Data corrected for STP.

Due to the tests having been conducted outdoors, environmental variables such as the wind could have contributed to the erratic arc direction by blowing out the plasma channel. Figure 24 shows arcs that occurred in opposite directions, however, there was no noticeable change in the direction of the wind during the tests.

The supply current was only measured during the initial setup tests and not for the individual flashover tests. A measure of the supply current could have assist in furthering the understanding of the difference in breakdown mechanism. A large surge in current immediately before flashover is indicative of leader the mechanism, while a gradual increase (but to a lower maximum magnitude) is indicative of the streamer mechanism.

Given that the point electrode and protrusion was in corona, it is also likely that there was space charge present in the vicinity of the test objects. The presence of the space charge could have randomly changed the electric field magnitude and thereby contributed to erratic observations of the arc discharge path.

7.4 The Presence of the Sphere and the Reduction in the Insulation Strength

The tests conducted showed a generally constant flashover-voltage irrespective of the position of the floating object. Using the characteristic linear equation shown in Figure 23, it was calculated that the breakdown voltage of the gap with the floating object was approximately the same as a smaller gap without the sphere.

The ratio of the gap size to the sphere diameter may not directly represent a live worker in practical situations. The size of the sphere may therefore impact the breakdown voltage. A smaller sphere in the same gap or a large gap size may result in a different trend. Such research can be considered for future further investigation.

The raised ridge around the diameter of the sphere was an area of concern as it may affect the space potential around the sphere and air gap. From the results obtained it is concluded that this raised area did not have a significant effect on the tests as the images from the corona camera do not indicate any discharge activity on or around it, nor were there any direct flash overs noted from that region of the sphere.

7.5 Altitude Correction

Substantial information has been published on the electrical breakdown of air gaps, however, there is little data relating to comparisons for high altitudes and/or large air gaps. In 2013, the author conducted experiments investigating altitude correction factors under HVDC voltage [22]. The following were concluded from the investigation:

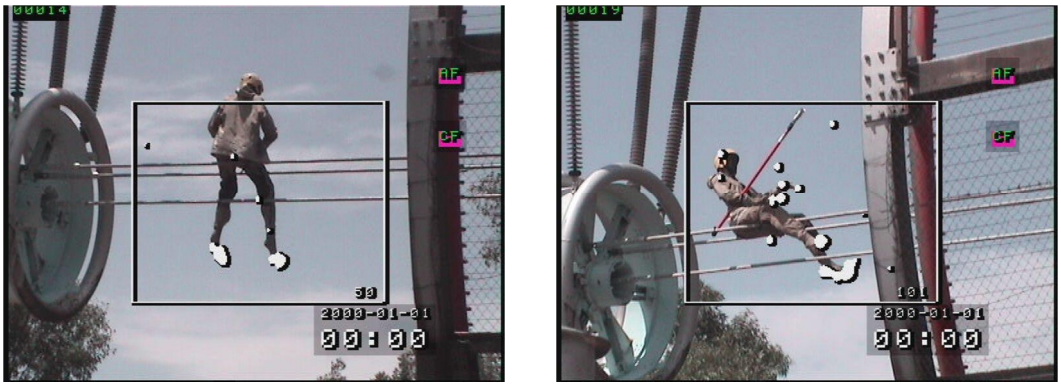
- Caution needs to be exercised when using IEC corrected test data from laboratories at low altitudes to predict dc flashover-voltages at high altitudes.
- The results of this work are in agreement with Calva et al [23][24] that there are some discrepancies when using the IEC 60060-1:2010 correction for dc voltages at high altitudes.
- The effect of other environmental variables such as wind and humidity on the flash-over-voltage needs to be understood.

The data analysed in this research report was corrected for STP using the existing IEC 60060-1 standard. It is acknowledged that the results require further analysis in respect of these findings. This, however, is not the included in the scope of this research report as consensus and agreement still needs to be obtained on new standards.

7.6 Static Charging of the Floating Object

As seen in Figure 43, the floating object can become statically charged. The charge resulted in corona discharges on the surface of the sphere, and not necessarily at the protrusion tip. As postulated in section 6.1.1, the space charge around the tip of the protrusion could have a shielding effect for corona discharges.

Depending on the magnitude of the static charge, the fields around all sharp points could become sufficiently high to cause ancillary corona activity. As an example, Figure 47 shows a separate test, using a mannequin dressed in a conductive live work suit. The mannequin was situated on a transmission line in expected work positions and energised with dc voltage. A corona camera was used to detect discharge activity.



(a) (b)

Figure 47: CoroCAM® images of discharge activity on live working mannequin

Although directly charged by the transmission line itself, evident in the Figure 47, are the areas susceptible for corona discharges (viz. the workers hands and feet). Should the live worker be approaching the transmission line (e.g. suspended under a hovering helicopter directly above a live line), and if he/she becomes charged to an equivalent level, then it is likely that the same areas of their body will exhibit corona activity. In this particular configuration, discharge activity was detected at line voltages as low as +145 kV. Although no direct relation can be drawn, relating to the equivalent expected charging of the worker, it is noted that such discharge activity is undesirable. As noted in [5,6], given suitable conditions (i.e. hot, low humidity, no space charge, and suitably high background electric fields) an anomalous flashover could occur. It is also noted that for the floating object tests, the sphere was electrically discharged after each flash.

8. Conclusion

Air breakdown for large air gaps under positive voltage stress is consistent and repeatable. For all cases (viz. point-to-plane and with the floating object) the deviation was less than 5% between successive flashover tests. The negative case is less repeatable. This is attributed to the differences in the physical breakdown processes occurring at the electrically stressed electrodes and the associated probability of free electrons being excited and ionised.

It has been observed that for positive polarity a lower voltage is required to breakdown a fixed gap size, when compared to negative polarity. This result was as expected and is in agreement with published literature. This is attributed to the different physical breakdown processes occurring at the electrically stressed electrodes.

The electrical breakdown characteristic of large air gaps (i.e. greater than 1 m) under positive HVDC has been determined for the specific point-to-plane geometry tested. Unfortunately, due to limitations with the power supply, large air gaps could not be evaluated under negative polarity.

Presently, HVDC live working is done using the ac techniques as the reference. Further, calculations of the minimum approach distance is done using extrapolations of ac test data. This research has shown that there are differences in breakdown behaviour in both positive and negative polarity cases. Further, the presence of the floating object does reduce the insulation strength of the air gap. In this work, for this particular gap configuration the reduction was as high as 70%. The applicability to practical situations still needs to be established, but it may be concluded that live work calculations need to consider this reduction factor when developing applicable live working standards.

For this work the gap sizes are considered small and it is unlikely that the leader breakdown mechanism was observed. Due to the relatively small length of the gaps being evaluated, it was expected that the streamer mechanism to be prevalent, but the observations of the erratic arc behaviour suggests that other issues related to environmental effects as well as space charge may have also contributed to it.

The static dc tests results are different than that obtained from impulse voltages and the presence of the floating object has shown to significantly decrease the flashover-voltage of a large gap. For HVDC transmission line maintenance, the static voltage case is the

predominant scenario that live workers will be exposed to, this must be carefully considered with regard to the interpretation and calculation of MAD and safe working clearances.

Humidity does have an effect on the flashover-voltage under HVDC conditions. Unlike ac, under dc voltage stress, corona activity is enhanced during hot and dry conditions [27]. This has a major impact on live work as it is done predominantly and preferably in such conditions. The humidity effect is due to the fact that water vapour has an affinity for electrons. The free electrons generated by corona discharge activity are easily attached to the water vapour and do not contribute to further avalanche activity.

The analysis of the data obtained through this research has been done in accordance with IEC 60060-1 [18]. At the time of writing this report, it is known that the Cigré working group D1.50 is reviewing the correction factor calculations process as detailed in [18]. In addition, based on the limited test work done in [27], it is understood that there may be some discrepancies applicable to the dc aspect of correction factor calculation. It is thus acknowledged that there may be errors introduced into the analysis due to the uncertainties with the IEC 60060-1 conversion process.

Floating objects in non-uniform dc fields may become highly statically charged. In relation to live working, all sharp areas around the worker body can initiate streamers. Given the right surface gradients, space potential, altitude and humidity conditions, these could develop into leaders or the sufficiently high field could cause the streamers to bridge the safe clearance space.

9. Recommendations

Negative polarity generally requires a much higher voltage to cause flashover. This work was unable to test this case and make a comparison with the positive polarity results. Larger air gaps need to be tested to draw definite conclusion relating to practical situations (3 to 5 m air gaps with floating objects). This would require a power supply in the MV range. It is recommended that this work be concluded at a test facility that will allow for higher dc voltages. There is currently no such test facilities in South Africa.

In order to determine the exact breakdown mechanism at play, additional investigations will need to be done. Firstly, the dc current needs to be measured and secondly, the breakdown can be recorded using a high-speed camera.

The electrostatic charge on the floating object could be investigated in order to bring further insight into the discharge mechanisms occurring in the secondary gap.

10. References

[1] E. Kuffel, W.S. Zaengl, J. Kuffel, “High Voltage Engineering Fundamentals”, Second edition, Butterworth-Heinemann, ISBN: 0 7506 3634 3, London, 2000.

[2] G. Gela, “Spark over performance and gap factors of air gaps below 1 meter,” Electric Power Research Institute – TR 106335, Lenox MA, 1998.

[3] F.A.M. Rizk, “Effect of floating conducting objects on critical switching impulse breakdown of air insulation,” IEEE transactions on Power Delivery, Vol. 10 No. 3, 1995.

[4] G. Gela, “EPRI Live Working Reference Book”, Second edition, Electric Power Research Institute, Reference no: 1024479, November , 2011.

[5] R Wachal, “Unexplained Nelson River HVDC flashovers”, Manitoba HVDC Research Centre, Centre Journal, Volume 11 Issue 4, Winter 2000, pp 1.

[6] D.W. Miller, B.D. Randall, O.C. Norris-Elye, ”Anomalous flashovers on the Nelson River HVDC transmission line”, Canadian Electrical Association – Power system operation and planning section - Insulation co-ordination subsection, Toronto, March 1989.

[7] “Transmission Ten Year Development Plan for 2011-2020”, Eskom Holdings SOC Ltd, 2011. Website reference: http://www.eskom.co.za/Whatweredoing/TransmissionDevelopmentPlan/Pages/Transmission_Development_Plans.aspx, last accessed 20 September 2013.

[8] Eskom Power Series, “HVDC Power Transmission – Basic Principles, Planning and Converter Technology (Part 1)”, Crown Publications, ISBN 978-0-9921781-0-9, Johannesburg, 2012.

[9] “HVDC - Connecting to the Future”, Second Edition, Alstom Grid, France, 2011.

[10] E. F. Raynham, “Apollo - Cahora Bassa: Enigma and Diversions”. EE Publishers, Johannesburg 2004.

[11] P.V. Goosen, “Southern African HVDC”, Presentation: Elia/50 Hz Meeting, Johannesburg, 18 January, 2013.

[12] Website reference: “Mozambique invites consultancy bids for CESUL project” http://www.globaltransmission.info/archive.php?id=14467, Last accessed January 25, 2014

[13] R. Silcock, “Live maintenance of high voltage transmission lines – Safety is paramount”, ABB Ltd, New Zealand, Website reference: http://www02.abb.com/global/gad/gad02077.nsf/lupLongContent/5975E947217CDC92C1256EFA0048910E”. Last accessed 16 February 16 February 2014.

[14] G. Sibilant, G. Gela, “High Voltage Direct Current live line and insulator testing”, Electric Power Research Institute – Report No: 1021957, Palo Alto, CA, December, 2011.

[15] P. S. Maruvada, "Corona on Transmission systems: Theory, design and performance", Eskom Power Series ISBN: 978-0-620-49388-8, Crown Publications, 2011.

[16] Department of Labour, Republic of South Africa, "Occupational Health and Safety Amendment Act, No181", 1993.

[17] IEEE Std. 516, "IEEE guide for maintenance methods on energised power lines", E-ISBN : 978-0-7381-5911-9, 2009.

[18] IEC 60060-1, "High Voltage Test Techniques – Part 1: General definitions and test requirements". Edition 2, 1989.

[19] R. Lings, "EPRI AC transmission line reference book – 200 kV and above", Third edition, Electric Power Research Institute – Report No: 1011974, Palo Alto, CA, December, 2005.

[20] N. Parus, N. Mahatho, T. Govender, H.A. Roets, J. Badenhorst, J.P. Reynders: "Results obtained during gap testing under HVDC conditions", Eskom Research Report: RES/RR/09/31452, 2010.

[21] N. Mahatho, G.C. Sibilant, and A.C. Britten, "The influence of artificial floating metal objects on the breakdown of air gaps under DC voltage," IEEE PES HVDC Congress - UKZN, June, 2006.

[22] N. Parus, I.R. Jandrell, N. Mahatho, T. Govender, H.A. Roets, "Live work under HVDC voltage: An investigation into altitude effects of flashover-voltage for rod-plane air gaps", 18th International Symposium on High Voltage Engineering, Seoul, South Korea, August, 2013.

[23] P.A. Calva, V. Moral, M.G. Del, Márquez, G.P Cabrera, "New proposal of correction factors for dc voltages", Conference on Electrical Insulation and Dielectric Phenomena, 2003. Annual Report, 2003, Page(s): 455 – 458.

[24] P.A. Calva, F.P Espino, "Correction factors for positive dc voltages", IEEE Transactions on Dielectrics and Electrical Insulation, Volume: 5, 1998, pp: 541 – 544.

[25] J.S. Townsend, "Electricity in gases", London, Oxford University Press, 1915.

[26] L. Niemeyer, L. Ullrich, and N. Wiegart, "The mechanism of leader breakdown in electronegative gases," IEEE Transactions on Electrical Insulation Vol. 24 No.2, April 1989, vol. 24, no. 2, pp. 309 - 324, April 1989.

[27] N. Parus, H.A. Roets, N. Mahatho, T. Govender, "The effect of altitude, temperature and humidity on corona inception and audible noise under HVDC voltage stress", Eskom Research Report: RES/PU/13/35174, Eskom Holdings SOC Ltd, Johannesburg, March 2013.

[28] Website reference: http://srirajkumar.files.wordpress.com/2011/06/unit-2.doc, last accessed 1 March 2014.

11. Appendices

11.1 Appendix A: Point-to-Plane Test Results (Positive and Negative Polarity)

TEST 1:	POINT TO PLANE	**REL HUMIDITY:**	30.5	%
VOLATGE:	POSITIVE	**TEMP:**	21.3	Deg. C
GAP SIZE:	1 m	**ATMOS PRESS:**	851.7	mbar

	Raw Data (kV)	**Corrected for STP (kV)**
Flash 1	388.9	492.2
Flash 2	384.6	486.8
Flash 3	376.1	476.1
Flash 4	384.6	486.8
Flash 5	377.5	477.9
Minimum:	376.1	476.1
Average:	382.3	484.0

TEST 2:	POINT TO PLANE	**REL HUMIDITY:**	30.5	%
VOLATGE:	POSITIVE	**TEMP:**	22.2	Deg. C
GAP SIZE:	1.25 m	**ATMOS PRESS:**	851	mbar

	Raw Data (kV)	**Corrected for STP (kV)**
Flash 1	509.0	644.4
Flash 2	504.8	639.0
Flash 3	502.0	635.4
Minimum:	502.0	635.4
Average:	505.3	639.6

TEST 3:	POINT TO PLANE	**REL HUMIDITY:**	46.6	%
VOLATGE:	NEGATIVE	**TEMP:**	19.5	Deg. C
GAP SIZE:	0.42 m	**ATMOS PRESS:**	849.7	mbar

	Raw Data (kV)	**Corrected for STP (kV)**
Flash 1	395.9	471.3
Flash 2	339.4	404.0
Flash 3	335.1	399.0
Flash 4	321.0	382.1
Flash 5	322.4	383.8
Minimum:	321.0	382.1
Average:	342.8	408.0

11.2 Appendix B: Positive Polarity Floating Sphere Test Results

			BREAK DOWN VOLTAGE (+ kV)						Minimum Voltage	STP correction	Average Voltage	Average STP Corrections	Standard Deviation	Temp	Relative Humidity	Atmospheric Pressure
	Total Gap Size (m)	Primary Gap Size (m)	Flash 1	Flash 2	Flash 3	Flash 4	Flash 5	Flash 6						(Deg. C)	(%)	(mbar)
Test 1	**1**	**0.1**	275.7	270.1	274.3	268.7	272.9	272.9	268.7	340.1	272.4	344.8	2.63	19.2	33	852
Test 2	**1**	**0.2**	282.8	282.8	272.9	274.3	274.3	274.3	272.9	345.4	276.9	350.5	4.60	19.2	33	852
Test 3	**1**	**0.3**	277.1	277.1	277.1	-	-	-	277.1	350.8	277.1	350.8	0.00	19.2	33	852
Test 4	**1**	**0.4**	275.7	275.7	275.7	-	-	-	275.7	349.0	275.7	349.0	0.00	19.2	33	852
Test 5	**1**	**0.5**	282.8	282.8	282.8	-	-	-	282.8	358.0	282.8	358.0	0.00	19.2	33	852
Test 6	**1.25**	**0.1**	367.6	367.6	367.6	-	-	-	367.6	465.4	367.6	465.4	0.00	19.2	33	852
Test 7	**1.25**	**0.2**	373.3	377.5	371.9	-	-	-	371.9	470.7	374.2	473.7	2.94	19.2	33	852
Test 8	**1.25**	**0.3**	374.7	367.6	373.3	-	-	-	367.6	465.4	371.9	470.7	3.74	19.2	33	852
Test 9	**1.25**	**0.4**	388.9	381.8	381.8	376.1			376.1	476.1	382.1	483.7	5.21	19.2	33	852
Test 10	**1.25**	**0.5**	373.3	376.1	379.0	-	-	-	373.3	478.6	376.1	482.2	2.83	20.6	27.6	850
Test 11	**1.25**	**0.6**	381.8	383.2	383.2	-	-	-	381.8	489.5	382.7	490.7	0.82	20.6	27.6	850
Test 12	**1.25**	**0.7**	397.3	391.7	395.9	-	-	-	391.7	502.2	395.0	506.4	2.94	20.6	27.6	850
Test 13	**1.4**	**0.9**	466.6	480.8	475.1	-	-	-	466.6	598.2	474.2	607.9	7.12	20.6	27.6	850
Test 14	**1.4**	**0.8**	461.0	467.0	460.0	-	-	-	460.0	589.7	462.7	593.2	3.79	20.6	27.6	850
Test 15	**1.4**	**0.7**	445.4	444.0	452.5	438.3			438.3	562.0	445.1	570.6	5.82	20.6	27.6	850
Test 16	**1.4**	**0.6**	431.3	444.0	441.2	-	-	-	431.3	552.9	438.8	562.6	6.68	20.6	27.6	850
Test 17	**1.4**	**0.5**	435.5	427.0	424.2	-	-	-	424.2	550.9	428.9	557.0	5.89	21	25.4	849
Test 18	**1.4**	**0.4**	424.2	424.2	421.4	-	-	-	421.4	547.2	423.3	549.7	1.63	21	25.4	849
Test 19	**1.4**	**0.3**	417.1	429.9	420.0	-	-	-	417.1	541.7	422.3	548.5	6.68	21	25.4	849
Test 20	**1.4**	**0.2**	425.6	428.4	428.4	-	-	-	425.6	552.7	427.5	555.2	1.63	21	25.4	849
Test 21	**1.4**	**0.1**	425.6	418.5	422.8	-	-	-	418.5	543.6	422.3	548.5	3.56	21	25.4	849

11.3 Appendix C: Negative Polarity Floating Sphere Test Results

			BREAK DOWN VOLTAGE (- kV)						Min Voltage	STP correction	Average Voltage	Average STP Correction	Standard Deviation	Temp	Relative Humidity	Atmospheric Pressure
	Total Gap Size (m)	Primary Gap Size (m)	Flash 1	Flash 2	Flash 3	Flash 4	Flash 5	Flash 6						(Deg. C)	(%)	(mbar)
Test 1	**1**	**0.1**	431.3	431.3	431.3	-	-	-	431.3	519.6	431.3	519.6	0.00	19.5	46.6	849.7
Test 2	**0.75**	**0.1**	353.5	367.6	387.4	381.8	411.5	-	353.5	425.9	380.4	458.3	21.81	19.5	46.6	849.7

11.4 Appendix D: Publication at ISH 2011

XVII International Symposium on High Voltage Engineering, Hannover, Germany, August 22-26, 2011

PRELIMINARY RESULTS OF AN INVESTIGATION INTO THE EFFECTS OF FLOATING OBJECTS ON THE ELECTRICAL BREAKDOWN OF AIR UNDER HIGH VOLTAGE DIRECT CURRENT STRESS

N. Parus[1&2*], I.R. Jandrell[2], J.P. Reynders[2], N. Mahatho[1&2],
T. Govender[1&2] and H. A. Roets[3]
[1]Eskom Holdings SOC Ltd, Johannesburg, South Africa
[2]The University of the Witwatersrand, Johannesburg, South Africa
[3]Kiepersol Technology, Johannesburg, South Africa
*Email: nishanth.parus@eskom.co.za

Abstract: The South African Power Utility, Eskom, has indicated its intent to possibly construct new High Voltage Direct Current (HVDC) schemes. An aspect that must be considered during the feasibility study for such projects is the live line maintenance of the transmission lines. The air breakdown mechanism under HVDC conditions when considering live work and tower geometries, must be properly understood before live work may be performed. Experimentation using floating objects is often used to study the effects relating to live work in high voltage applications. This paper presents the results of HVDC air breakdown tests using a 300 mm diameter floating metallic sphere with a 30 mm protrusion, in a point-to-plane configuration with a total gap length ranging between 0.75 m and 1.4 m. Both positive and negative polarity cases were tested. The results indicated that the position of the floating sphere does not significantly affect the flashover voltage magnitude. There is, however, a definite reduction in the strength of the air gap, between 27% and 29%, for the cases tested. Further, the static charge on the floating object did not influence the breakdown voltage. There is also linearity in flashover voltages of simple point-to-plane air gaps.

1. INTRODUCTION

Eskom currently operates and maintains the South African section of the Cahora Bassa High Voltage Direct Current (HVDC) scheme. The nominal operating voltage of the scheme is ±533 kV. Further, there are plans to possibly implement additional ±600 kV or ±800 kV HVDC schemes within the country.

There is a high availability requirement for the Cahora Bassa scheme and this may be required for the new DC schemes as well. Currently, live work is not being performed at full system voltage. Long downtime durations for maintenance cannot be sustained and live work is becoming more critical. Further, proactive live maintenance tends to reduce potential outages.

It is generally accepted that there are some differences in the air breakdown mechanism under HVDC conditions to that of High Voltage Alternating Current (HVAC) [6,8], in particular the influence of space charge and the manner in which streamer development is initiated. These issues must be carefully considered before live work can be performed safely on the DC lines. These issues include the impact of space charge in the vicinity of the live worker, the air breakdown mechanism for the different polarity transmission lines, electrical behavior of a floating object in the air gap, correct minimum approach distance (MAD) factors and the risk of flashover (ROF) under HVDC and EHVDC conditions.

This paper focuses on the aspects pertaining to the behaviour of metallic floating objects under HVDC conditions. Floating metallic spheres are often used in experimentation to understand the behaviour of air gaps under high voltage applications.

2. HYPOTHESIS

Floating objects (whether metallic or not) that are positioned within a DC electric field will affect the average field distribution. The perturbation of the electric field may affect the characteristics of the electrically stressed air gap. If the floating object represents a live worker's approach to the HVDC transmission line/conductor bundle or to any of the hardware attachments on the line, its presence is likely to intensify the electric field and increase the risk of flashover.

It is reported that under switching impulse conditions there is a marked decrease in the flashover voltage when the floating object is positioned towards the centre of the air gap [5]. Under DC conditions the electrical charging of the floating object and space charge effects may result in a different trend.

This paper thus investigates the influence of a metallic floating object on DC breakdown voltage in a point-to-plane configuration.

The picture below shows an example of a live line worker being lowered onto the Cahora Bassa transmission line by a helicopter and is an example of a practical situation where the HV lines could be affected by floating objects.



Figure 1: Live worker being lowered onto the conductor

3. EXPERIMENTAL SETUP

The test setup involved placing a 300 mm diameter metallic sphere, with a 30 mm protrusion facing the earth plane, in different positions within a point-to-plane air gap ranging from 0.75 m to 1.4 m.

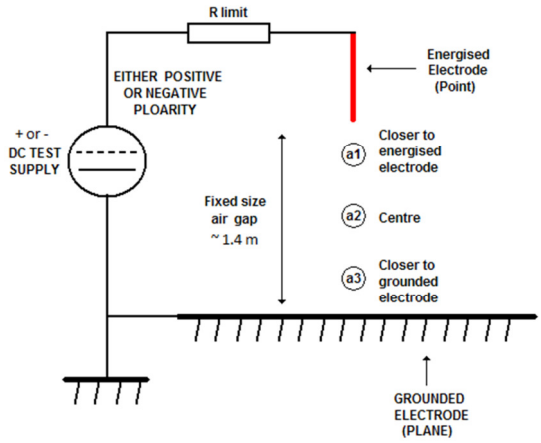


Figure 2: Schematic diagram of the test setup

The sphere was positioned in various places within the gap (as indicated from a1 to a3 in Figure 2). A 30 mm protrusion was implemented on the bottom of the sphere to replicate practical situations where it is difficult to maintain smooth surfaces. The presence of the protrusion results in a lower breakdown and may suppress the accumulation of free charge on the sphere [5].

The power supply consisted of a ±500 kV DC (15 mA), half wave rectified source. The rectifier was supplied by a 400 kV AC transformer. The diode stack was protected by a current limiting water resistor. Ripple voltage smoothing was provided by existing coupling and measuring capacitors that are used for AC corona cage research.

The metallic sphere was suspended between two 2 m substation post insulators, with nylon string. A grounded wire mesh was placed below the sphere. A copper pipe was used to create the point as shown in Figure 4. The tests were conducted outdoors.

3.1 Test circuit

The electrical representation of the test circuit used was as follows:

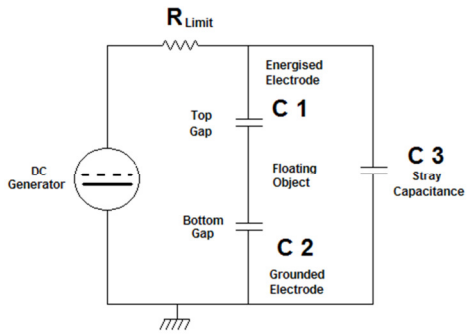


Figure 3: Schematic representation of the test circuit

Figure 4 is a picture of the experimental setup.

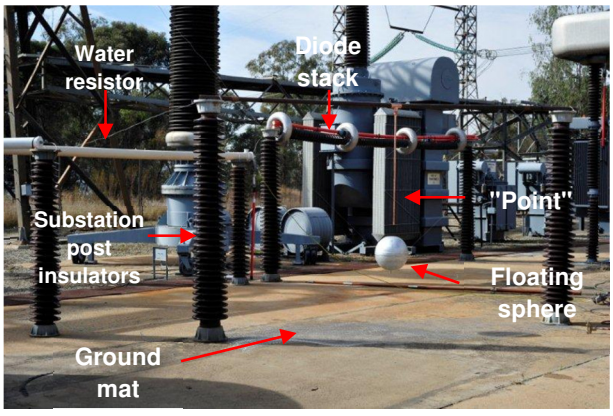


Figure 4: Photograph of the test setup

The test were conducted in accordance with the IEC60060-1 standard [1], and corrected per accepted industry practices for Standard Temperature and Pressure (STP) as well as for humidity.

3.2 Test methodology

Firstly, the flashover voltage of a point-to-plane air gap (without the sphere) was determined for reference purposes. The total gap size was determined by the maximum voltage that could be practically flashed over using the 500 kV source. Once the total gap size was set, positive DC voltage was applied to the 'point' and the voltage was slowly raised until a flashover occurred. The flashover tests were repeated between three and seven times at each position to determine the repeatability. A time delay of one minute was allocated between each test.

Secondly, the sphere was inserted into the air gap, close to the point source, and the flashover tests were repeated. The position of the sphere was then systematically adjusted until it approached the ground plane. After a series of tests, the total gap size was reduced and the procedure was repeated.

On completion of the positive polarity tests, negative voltage was applied to the point source and the procedure was repeated.

4. TEST RESULTS

4.1 Flashover voltage of a point-to-plane air gap

The following results are corrected for STP as per [1]:

Table 1: Results for positive polarity

POSITIVE POLARITY	AVERAGE FLASHOVER VOLTAGE (kV)	MINIMUM FLASHOVER VOLTAGE (kV)
1.00 m air gap	484	476
1.25 m air gap	640	635

It was not possible to flashover the 1.4 m air gap using the 500 kV test power supply.

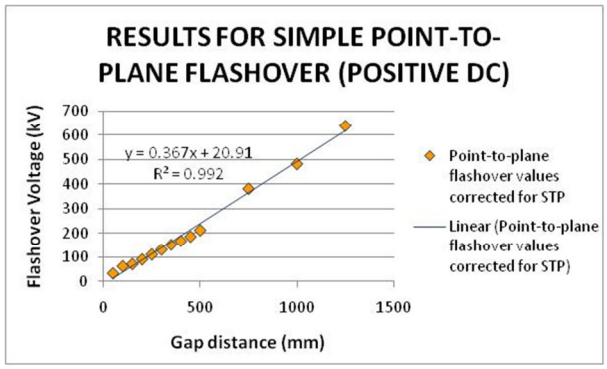


Figure 5: Graph showing linearity for positive polarity DC flashovers

When plotted together with data from previous gap testing conducted by the authors [3], a linear trend was observed for the range of point-to-plane gaps tested.

Negative polarity DC generally requires a higher voltage level to flashover the same size air gap

than positive DC [2,3,4]. The power supply only allowed for the safe testing of a 0.42 m air gap.

Table 2: Results for negative polarity

NEGATIVE POLARITY	AVERAGE FLASHOVER VOLTAGE (kV)	MINIMUM FLASHOVER VOLTAGE (kV)
0.42 m air gap	408	382

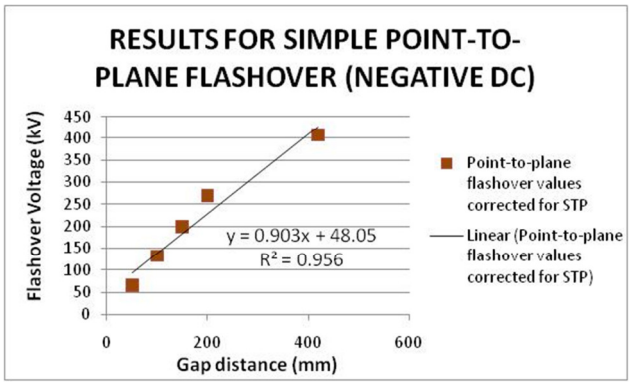


Figure 6: Graph showing linearity of negative polarity DC flashovers

When plotted together with data from previous gap testing conducted by the authors [3], a fairly linear trend was observed for the range of point-to-plane gaps tested.

4.2 Flashover voltage of a floating metallic sphere

The following results were obtained:

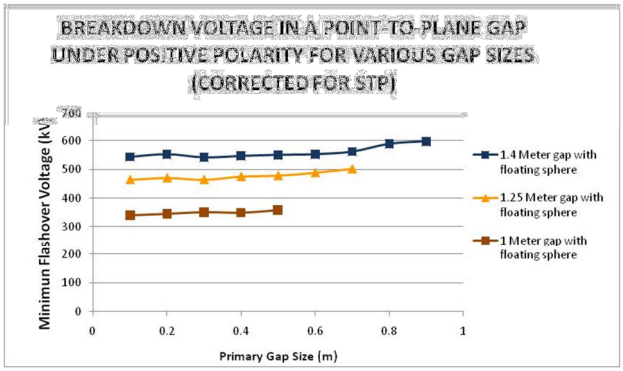


Figure 7: Graph showing results for positive polarity floating object tests

The flashover voltage was constant for the positive polarity case. For the smaller total gap size the position of the sphere did not impact the flashover voltage. It was observed that the flashover voltage had a tendency to increase as the primary gap became larger.

Only two test positions were possible for the negative polarity case. This was due to the limitations of the power supply and the size of the total gap.

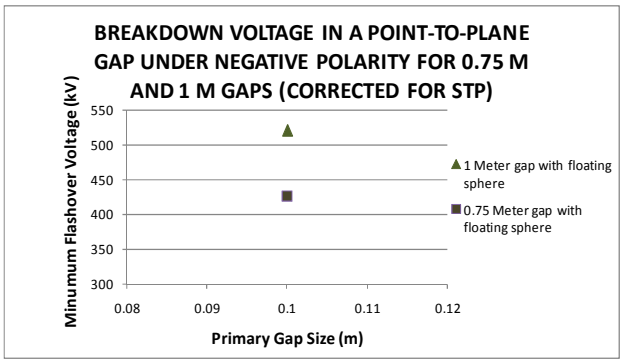


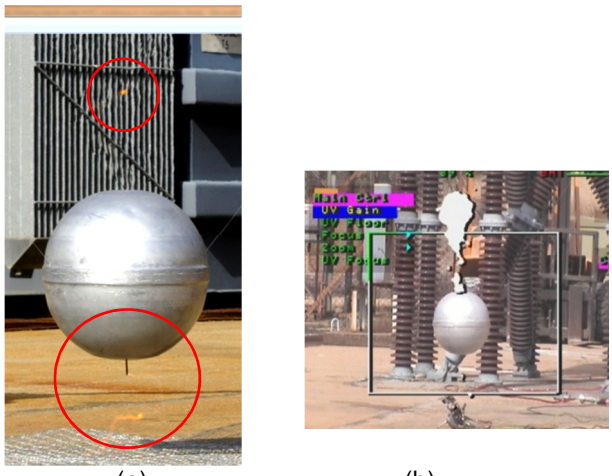
Figure8: Graph showing results for negative polarity floating object tests

4.3 Reduction in air gap strength

The presence of a sphere in the air gap results in a definite reduction of the air gap insulation strength. For the positive case, in a 1 m gap, the gap strength is reduced by 109 kV, indicating a 29% decrease. For the 1.25 m gap, the flashover voltage is reduced by 133 kV, a 27 % decrease. No results were obtained for the negative case.

4.4 Observations during the tests

For the larger gaps, the emitted electromagnetic energy was visible in the primary and secondary gaps. For certain tests, visible and ultraviolet (UV) discharges were observed in the gap without the presence of a clear arc.

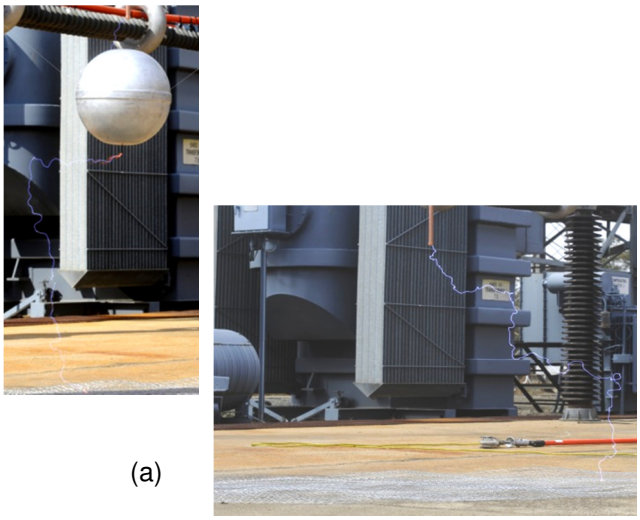


(a) (b)

Figure 9: (a) Visible electrical discharges in the secondary gap **(b)** UV discharges in the gap - No evidence of a complete flashover of the primary gap.

UV images taken using a CSIR CoroCam® (Figure 9 b) indicate discharge behaviour before the complete flashover occurred. Visually, the electromagnetic energy caused refraction of the light in the gaps resulting in wavy images being recorded. This is evident in the distorted image of the transformer cooling fins in Figure 9 a.

In many cases, the arc did not follow a straight or direct path between the electrodes. Figure 10 shows the elaborate arc path within the gaps.



(a) (b)

Figure 10: (a) Arc path in presence of floating object **(b)** Arc path in a simple point-to-plane gap

In two cases it was observed that the arc ignored the floating object and terminated directly on the ground mat. The sphere was positioned in the centre of the gap. This was not expected as the total gap size was 1.4 m and would have required a significantly higher voltage than that recorded for these tests.

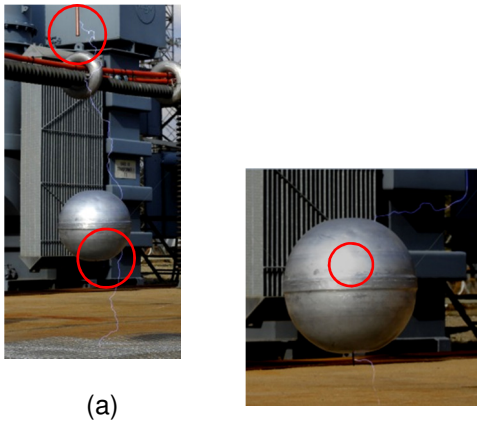


Figure 11: Arc missing the sphere to the right

In certain cases it was observed that the arc did not originate from the tips of the electrodes, but rather along its length. In the case of the sphere, the arc was observed to originate from the sides and not necessarily from the protrusion itself.

The current limit of the power supply was 15 mA. For practical HVDC lines the fault current is in the order of kilo-amperes. The energy discharge during these tests were considerably lower than what would be achieved on actual transmission lines and as such the arcs observed were considerably less intense (visually and audibly).

Initial tests included grounding the sphere after each flashover event to remove the trapped charge. Grounding between tests were compared to the case where the sphere was not grounded. It was noted that the sphere grounding process did not have an impact on the breakdown voltage and all further tests were done without discharging the sphere.



(a) (b)

Figure 12: (a) Arc originating on the sides of the rod and sphere **(b)** Arc originating on side of protrusion

Figure 13 indicates tortuous arc behaviour at the positive electrode. The picture was taken with a digital camera having a shutter speed of 0.12 ms. The image is therefore a sudo-steady state representation of the path taken by the electrons during the discharge.



Figure 13: Tortuous arc behaviour close to the energised rod (positive polarity)

Figure 14 shows a discharge at the bottom of the sphere and intense electromagnetic energy in the primary gap, even though there is no visible arc in the primary gap.

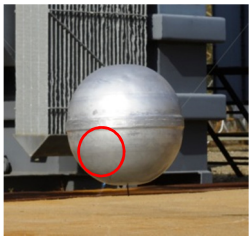


Figure 14: Electrical discharge activity on the side of the sphere

5. DISCUSSION

The maximum voltage of the test supply was 500 kV. This limited the maximum size of air gap that could be achieved. For positive polarity the maximum size of the air gap that could be safely flashed-over was 1.25 m. For the negative case, the largest gap was 0.75 m. For the same size of air gap, negative polarity requires a higher breakdown voltage than positive polarity. This was evident as illustrated in Figures 5, 6 and [2,3,6,7]. The power supply was unable to supply a high enough voltage to breakdown a larger gap. The test was stopped in order to protect the supply diodes from excessive current.

The voltage limitation did not allow for the replication of practical line and tower geometry gap sizes. Due to the scaling of the gap and floating object sizes, the tests therefore cannot be directly related to live working conditions.

Air breakdown is always initiated by streamer activity [7,8], however, for streamers to bridge the gap, the arc path taken is generally the shortest path between the electrodes (i.e. a straight line). The erratic arc path as observed during these tests may be an indication of a leader breakdown mechanism. Due to the tests having been conducted outdoors, wind could have contributed to the erratic arc direction by blowing out the plasma channel and or movement of space charges. Figure 10 shows arcs that occurred in opposite directions, however, there was no significant change in the direction of the wind during the tests.

Previous research using floating spheres under switching impulse conditions [5] indicated a distinct decrease in breakdown voltage for the sphere in the quartile of the gap closest to the high voltage electrode. The gaps tested in [5] were larger than that tested during this work and the voltage magnitudes were significantly higher. Further, switching impulses occur much quicker than constant DC and the mechanism of the air breakdown may be different.

The tests showed a generally constant flashover voltage irrespective of the position of the floating object. Using the characteristic linear equation shown in Figure 5, it was calculated that the breakdown voltage of the gap with the floating object was approximately the same as a smaller gap without the sphere (i.e. the total gap size less the diameter of the sphere and protrusion).

The ratio of the gap size to the sphere diameter may not directly represent a live worker in practical situations. The size of the sphere may therefore impact the breakdown voltage. A smaller sphere in the same gap or a large gap size may result in a different trend.

The negative polarity flashover voltage was more erratic and a higher standard deviation in the flashover voltages was recorded; 22 kV when compared to an average of 2 kV for the positive case.

6. CONCLUSIONS

The following conclusions are noted:

- There is a linear trend in flashover voltage for the rod-to-plane configuration for the ranges tested,
- The presence of the metallic floating sphere results in a 27-29% reduction in the strength of the air gap for the positive polarity case,
- The position of the sphere does not significantly affect the breakdown voltage value for this particular test configuration,
- The air gap can be stressed to an extent where there are electrical discharges within the primary and secondary gaps, without a complete flashover occurring,
- The charge on the floating object is important in determining the flashover of the primary air gap. Observations in certain cases revealed that the arc bypassed the sphere and terminated on the ground plane.
- Corona activity on the tips of the rod and the protrusion may result in a decrease of the local electric field strength. The arc then originated elsewhere on the rod or protrusion, a short distance away from the tip, where the local field was higher than at the tip,
- From these limited experiments, it appears that the behaviour of the breakdown of air gaps under sustained HVDC stress is different to that of switching impulses.

7. RECOMMENDATIONS

This research is the initial part of a greater study into the investigation of electrical breakdown of air under HVDC conditions. Although the exact dimensions of practical line and tower gaps could not be achieved due to limitations with the power supply, further work will be required with regard to gaining a better understanding of the test results obtained and their applicability to a representative live working condition.

Analysis of models of the breakdown of air that take into account space charge interaction as well as the static charge of the floating object must be compared to the empirical data obtained during

experimentation. Further research could include utilisation of a high speed video camera to understand the development of streamer and leader activity at the two electrodes, to repeat the tests for larger gap sizes, to consider different gap factors, and to investigate the effect of higher current discharges on the breakdown voltage.

8. ACKNOWLEDGMENTS

The authors would like to acknowledge Mr C. Esterhuizen for the digital video and photography and assistance with the test setup, and Mr A.C. Britten for his expert guidance and assistance in the project. The authors would also like to thank Eskom for the support of the High Voltage Engineering Research Group at the University of Witwatersrand, Johannesburg through the TESP programme. They would also like to thank CBI-electric, the department of Trade and Industry (DTI-THRIP) as well as to the National Research Foundation (NRF) for direct funding of the High Voltage Engineering Research Group at the University of Witwatersrand, Johannesburg.

9. REFERENCES

[1] IEC 60060-1, “High Voltage Test Techniques – Part 1: General definitions and test requirements”. Edition 2, 1989.

[2] G. Gela, “Sparkover performance and gap factors of air gaps below 1 meter,” Electric Power Research Institute – TR 106335, Lenox MA, 1998.

[3] N. Parus, N. Mahatho, T. Govender, H.A. Roets, J. Badenhorst, J.P. Reynders: “Results obtained during gap testing under HVDC conditions”, Eskom Research Report: RES/RR/09/31452, 2010.

[4] N. Mahatho, G.C. Sibilant, and A.C. Britten, “The influence of artificial floating metal objects on the breakdown of air gaps under DC voltage,” IEEE PES HVDC Congress - UKZN, June, 2006.

[5] F.A.M. Rizk, “Effect of floating conducting objects on critical switching impulse breakdown of air insulation,” IEEE transactions on Power Delivery, Vol. 10 No. 3, 1995.

[6] H.L Hill, A.S. Capon, O. Ratz, P.E. Renner, W.D. Schmidt, “Transmission line reference book: HVDC to ±600 kV", Project RP 104, EPRI, Palo Alto, CA, 2000.

[7] E. Kuffel, W.S. Zaengl, J. Kuffel, “High Voltage Engineering Fundamentals,” Second edition, Butterworth-Heinemann, ISBN: 0 7506 3634 3, London, 2000.

[8] P. S. Maruvada, "Corona on Transmission systems: Theory, design and performance.” Eskom Power Series ISBN: 978-0-620-49388-8, Crown Publications, 2011.

11.5 Appendix E: Publication at ISH 2013

August 25-30, 2013 | Seoul, Korea
ISH 2013 18th International Symposium on High Voltage Engineering

LIVE WORK UNDER HVDC VOLTAGE: AN INVESTIGATION INTO ALTITUDE EFFECTS OF FLASHOVER VOLTAGE FOR ROD-PLANE AIR GAPS

N. Parus[1*], I.R. Jandrell[1], N. Mahatho[1], T. Govender[1] and H.A. Roets[2]
[1]The University of the Witwatersrand, Johannesburg, South Africa
[2]Kiepersol Technologies, Johannesburg, South Africa
*Email: nishanth.parus@eskom.co.za

Abstract: Live line work on High Voltage Direct Current schemes is becoming more important due to increasing availability requirements of power systems. The direct current flashover voltage for a rod-plane air gap was studied at four different altitudes. The same test rig and equipment was used at all test sites. The values were corrected in accordance with IEC 60060-1:2010. Analysis of the results shows agreement with other independently published literature in that the IEC correction method does have some discrepancies for direct current voltages at high altitudes and/or large air gaps. It is concluded that caution needs to be exercised in using corrected data from test laboratories at low altitudes to predict direct current flashover voltages at high altitudes and/or large air gaps. This finding has an impact on transmission line design, the calculations used for determining live working minimum approach distances, safety clearances, etc. Further work has been proposed to better understand the discrepancies that have been found.

1 INTRODUCTION

Internationally, there are several High Voltage Direct Current (HVDC) schemes in operation, however, only a few of them conduct live work at full system voltage. Live line maintenance of such schemes is becoming more important as power utilities become faced with high availability requirements. As such, the air breakdown mechanism under HVDC conditions, where related to practical live working tower geometries, must be properly understood before live working may be undertaken. Internationally, experience with live work on HVDC lines is limited and little information is available on how minimum approach distance (MAD) values should be determined for HVDC live work. Furthermore, MAD values are based on extrapolations and do not account for significant differences between alternating current (ac) and direct current (dc) environments. This research has been initiated in order to understand the impacts that altitude has on these calculations.

Substantial information has been published on the electrical breakdown of air gaps, however, there is little data relating to comparisons for high altitudes and/or large air gaps. Initial results relating to this research topic considered floating objects in air gaps [1]. The results obtained were unexpected and required further analysis and explanation.

2 HYPOTHESIS

Electrical streamer onset voltage varies at different altitudes as it is dependent on the relative air density [2]. Under HVDC conditions, the presence of space charge has further influence in that it alters the electric field, effectively lowering the field gradient and suppressing further streamer activity. Generally, the International Electrotechnical Commission (IEC) standard 60060-1:2010 [3] is used to correct voltage values for altitude and temperature effects, however, the issue of the effect of space charge accumulation needs to also be considered.

For many utilities, live work is only conducted when the transmission line (and adjacent lines) is taken off the auto-reclose (ARC) protection feature and when there is fair weather (i.e. no thunder storm/lightning) visible. Since there is little risk of switching type over voltages, the main possibility of air breakdown is under steady state voltage conditions.

Rod-plane air gaps produce a non-uniform electric field distribution. This type of setup can be used to conduct experiments as it generally represents conditions that can be expected during live working situations (e.g., where a live worker is using tools in a stressed air gap, a live work platform or a robot with protruding arms).

3 METHODOLOGY

A portable rod-plane air gap was developed. The test setup was moved to four different test locations in South Africa, namely:

- Clarens (1880 m above sea level),
- Midrand (1500 m above sea level),
- Pietermaritzburg (822 m above sea level),
- Oribi Gorge (480 m above sea level).

These sites were selected as they were easily accessible by road and provided a safe area to erect the test equipment for the duration of the testing.

The rod was energised while the ground plane was solidly bonded to both the earth connection point of the HVDC power supply as well as an earth spike pegged in the ground. The gap length was varied between 50 mm and 700 mm at each test site. The voltage on the rod was manually increased at a rate of approximately 2kV/s, until flashover occurred. The test was repeated five times at each gap length. The measurements were limited to the maximum output of the dc generator (i.e. only 200 kV was attainable at some sites).

Only positive voltage was considered since the maximum voltage of the generator was 200 kV. This was not sufficient to allow negative flash-overs at the larger gaps or at low altitudes. At low altitudes, a higher negative voltage is required to flash over the gap, when compared to positive polarity for the same gap size.

Atmospheric variables such as temperature, relative humidity, wind speed and barometric pressure were recorded at each site. The flashover values were corrected using the process described in IEC 60060-1:2010 standard [3] and the results were analysed.

4 EXPERIMENTAL SETUP

The tests were initially proposed to be done using a pressure vessel at a fixed location. By varying the pressure within the vessel, results for different altitudes could be obtained. There were several challenges with regard to vessel size, bushing availability and pressurisation in using this technique. Instead, a simpler

portable test setup was developed. This revised technique involved transporting a portable air gap to various different locations. The solution allowed for quick erection of the test setup with the only challenge being the logistics of transporting the equipment to the identified test sites.

The experimental setup included a 12 V dc switch-mode uninterruptible power supply (UPS), HVDC power supply, resistive voltage divider, current-limiting water resistor and the rod-plane gap.

The test setup is shown in Figures 1 and 2. Two current-limiting water resistors, of approximately 2 MΩ each, were placed in series with the gap to limit the current drawn during flashover. The HVDC power supply was energised using a pure sine wave UPS. The voltage across the air gap was measured using a resistive voltage divider.



Figure 1: Rod-plane setup at 880 m above sea level (Pietermaritzburg). ***Note:*** the plane is elevated from ground-level

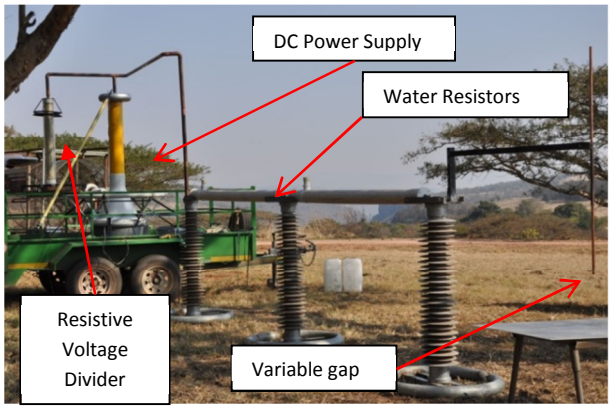


Figure 2: Rod-plane setup: Voltage divider, DC generator (yellow bushing) and water resistors

The rod was a 1.8 m long copper tube with a diameter of 16 mm. The ends were plugged using a copper end-cap. The plane was a 5 mm thick steel plate with a length of 1 m and a width of 0.8 m.

4.1 Elevation of the plane above ground

The earth plane was initially placed directly on the ground but it was observed that grass, dust and other debris was attracted to the electrodes (Figures 3 and 4). This resulted in anomalies in the results and it was therefore decided to elevate the earth plane above ground level to reduce the effect of the debris on the rod.

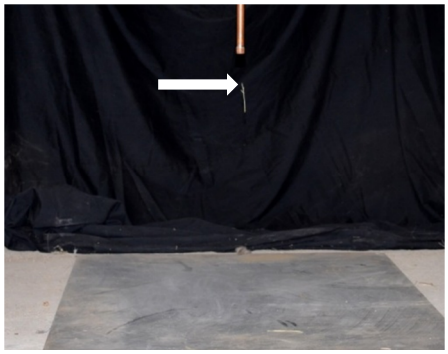


Figure 3: Electrostatic attraction of grass to the rod electrode.

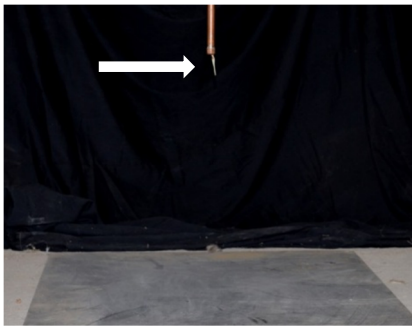
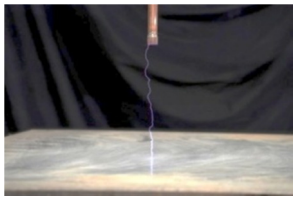
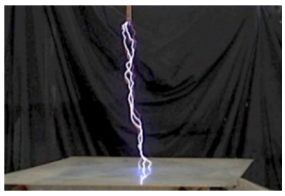


Figure 4: Electrostatic attraction of grass to the electrode.

For the purpose of these tests, the size of the plane was considered to be adequate since preliminary tests showed that all flashovers occurred to the centre of the plate and not to the edges (Figure 5).



(5 a)



(5 b)

Figure 5 (a): Flashover with a 200 mm gap (altitude 1500 m above sea level). (b) Multiple flashovers with a gap of 500 mm (Altitude 1500 m above sea level).

5 RESULTS

The five actual values per gap length are plotted in Figure 6. Figure 7 shows the results after corrections for air pressure, humidity and temperature are applied in accordance with [3].

The uncorrected results are closer to that expected, with regard to the linearity observed; however, there are discrepancies. Since the tests were conducted outdoors, the results are affected by wind and humidity. It is noted that the spread in the results at the respective gaps is wider in the gap range between 450 mm and 600 mm. There is approximately a 6% fluctuation in the recorded flash over voltage in this gap range (i.e. the voltage at which consecutive flash-overs occurred is not as consistent as at the other gap lengths).

The graphs for the corrected results are unexpected. If the correction procedure was applicable for the scenarios tested, then the data points for each gap length should ideally fall within close agreement with each other. This is not the case, as shown in Figure 7, as there is still a large spread at all gap sizes. In some cases the spread becomes larger after the correction is applied (viz. approximately 12% fluctuation in the recorded flash over voltage in the 400 mm to 600 mm gap range).

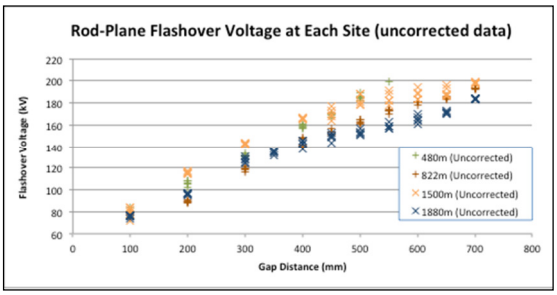


Figure 6: Uncorrected results for each site at different gap lengths

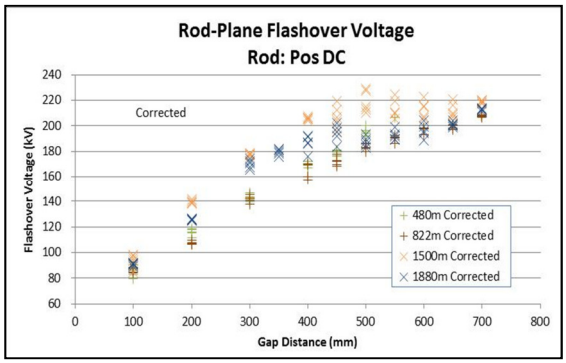


Figure 7: Corrected results for each site at different gap lengths

The uncorrected and corrected values for each site are depicted in Figures 8, 9, 10, and 11 respectively. For the Clarens results (Figure 8), very little differences were obtained in the corrected values except between the 400 mm and 600 mm gap range (i.e. the corrected values outside this range all lay within a close scatter). The same effect was found at an altitude of 1500 m (Midrand) (Figure 9), between the 450 mm and 650 mm range. This is unexpected as the uncorrected trends are more linear and the measurement points are more congruent outside this particular gap range. However, in both cases the spread in results at the 700 mm gap is very small.

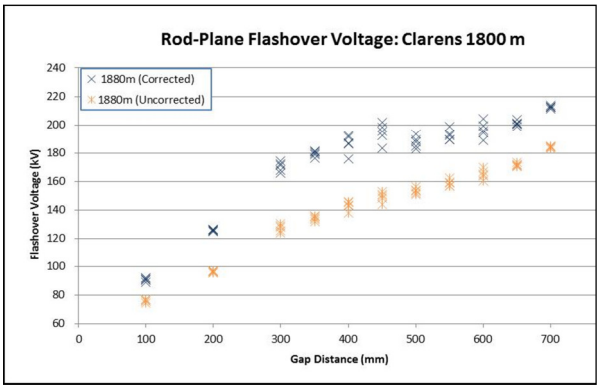


Figure 8: DC flashover voltages at an altitude of 1880 m (Clarens).

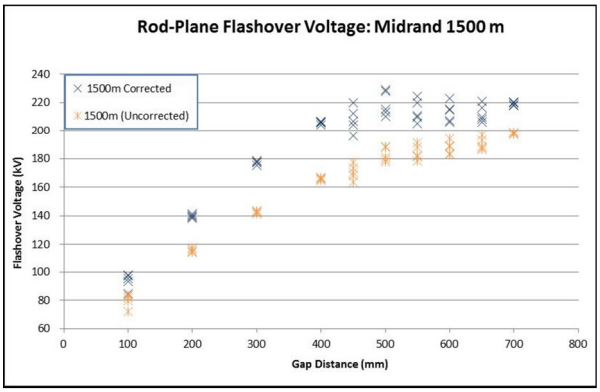


Figure 9: DC flashover voltages at an altitude of 1500 m (Midrand).

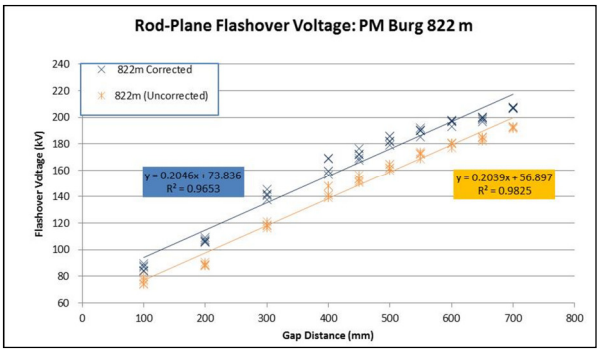


Figure 10: DC flashover voltages at an altitude of 822 m (Pietermaritzburg), with linear trend curves fitted.

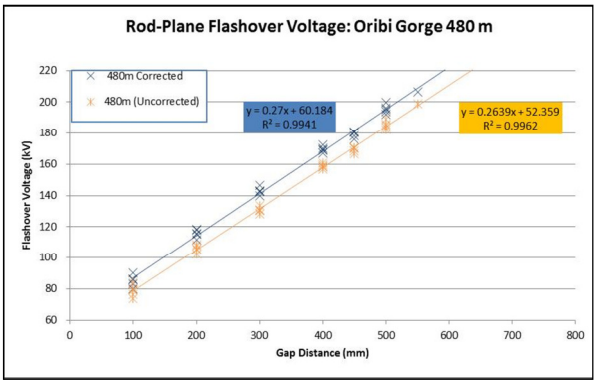


Figure 11: DC flashover voltages at an altitude of 480 m (Oribi Gorge), with linear trend curves fitted.

At the lower altitudes, 822 m and 480 m above sea level, the spread in the results at the respective gaps is considered small and there is an approximately linear relationship between the gap size and the flashover voltage.

For Figures 8, 9 and 10, the graphs seem to flatten towards the higher gap sizes. There is a distinct knee point at the gap of approximately 450 mm where the trend below exhibits a different linearity to the trend above.

The correction factor appears to be more accurate for the lower altitudes, 480 m and 822 m above sea level (Figure 12). The gap length at 480 m above sea level was limited to 550 mm. Due to limitations of the power supply only one flash was possible with this gap. Air gaps at low altitude have a higher electrical strength and the maximum voltage of the test supply was 200 kV. At this voltage heavy corona discharges were observed, however, the gap did not fully breakdown. At 822 m above sea level, the graph appears to flatten at the higher gap sizes (gold curve in Figure 12).

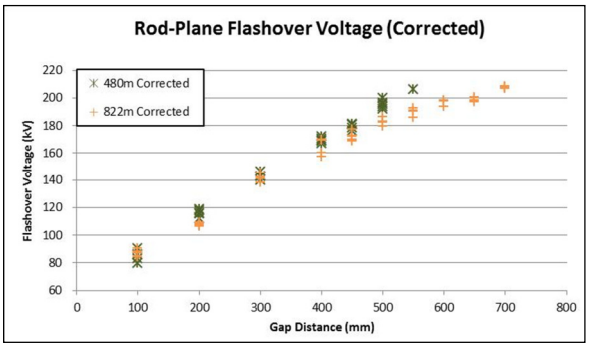


Figure 12: Comparing the corrected results for 480 m and 822 m.

The practical application for this research (i.e. live working) is for larger gaps. Thus only data from air gaps of 400 mm and more, and at the two high altitudes, are analysed in Figure 13.

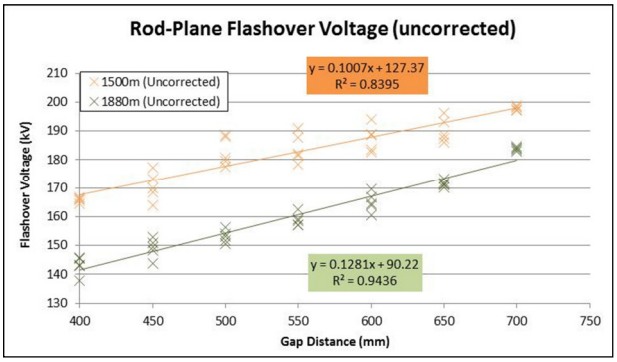


Figure 13: Comparing DC flashover voltages at 1500 m and 1880 m.

As previously mentioned, the larger gaps are characterised by a different linearity to that of the smaller gaps, so the results are analysed separately. It can be seen that the correction, between 1500 m and 1880 m, taking only altitude into consideration, is approximately 5.3 kV/100 m (20 kV/380 m). The uncorrected results from 822 m above sea level are anomalous as the values are expected to be higher than those from 1500 m but this is not evident in the trend (Figure 14).

The corrected values are also different to what was expected (Figure 15). Further, the corrected data points are more scattered than the uncorrected values.

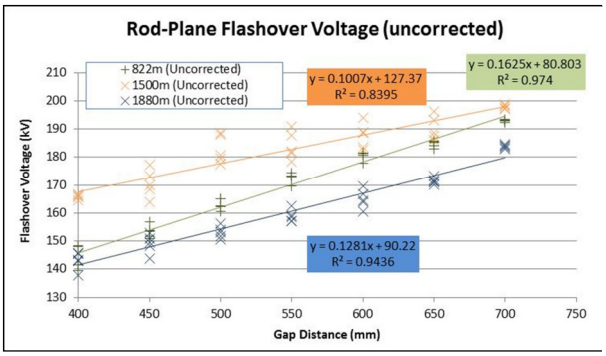


Figure 14: Comparing DC flashover voltages at 822 m, 1500 m and 1880 m.

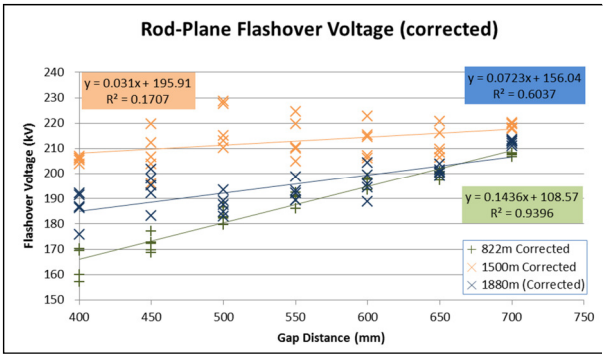


Figure 15: Comparing the corrected DC flashover voltages at 822 m, 1550 m and 1880 m.

The average, of the corrected values obtained for each gap length are depicted in Figure 16. If the correction method was correct, the curves in Figure 16 should have been straight lines. The results of bigger gaps (600, 650, and 700 mm) tend towards straight lines, with the Midrand values being slightly higher than expected. The spread in the measured values at all four measuring sites was small for the 700 mm gap, and produced a result closest to what is expected (i.e. a straight line).

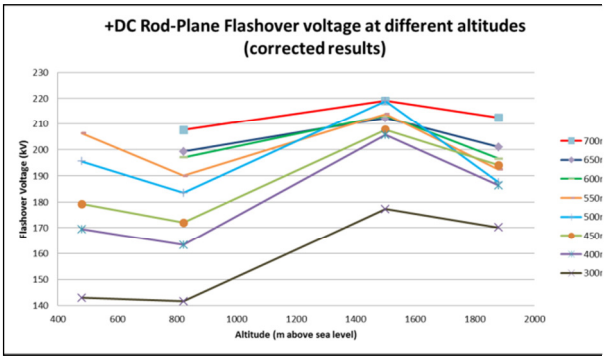


Figure 16: Comparing the effect of altitude on the DC flashover.

When analysing the uncorrected values, approximately straight lines are obtained between 822 m and 1500 m, at the larger gap sizes (Figure 17).

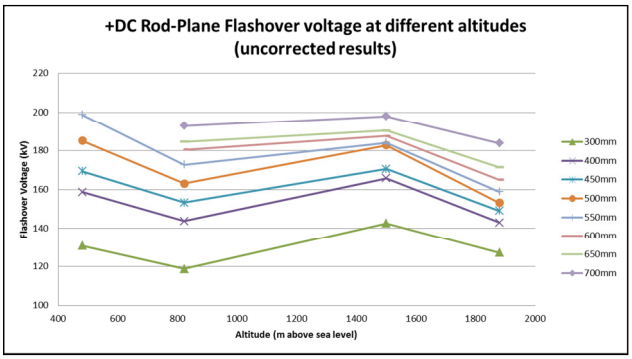


Figure 17: Comparing the effect of altitude on the average uncorrected DC flashover voltage

6 COMPARISON WITH OTHER PUBLISHED WORK

Results obtained from similar independent investigations are compared to the findings in this report. Allen et al in [4] performed similar measurements at Leatherhead in the United Kingdom, at altitudes less than 100 m above sea level. Reference [4] also lists the results obtained by Udo et al [5] of tests performed in Shiobara, Japan, at an altitude of about 600 m above sea level. In Figure 18, all these results are plotted together with the results obtained at 480 m above sea level (Oribi Gorge).

For the 400 mm gap, the Oribi Gorge data agrees with Allen et al [4]. For the 500 mm gap, the data is in agreement with Udo et al [5]. However, the slope of the South African data suggests much lower flashover voltages at the longer air gaps.

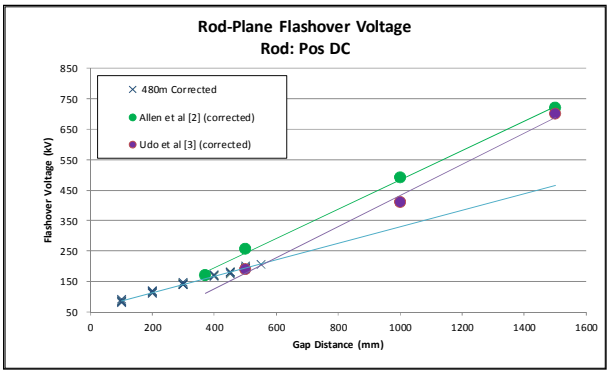


Figure 18: Comparison of the corrected South African results (at 480 m) with Allen [4] and Udo [5], with linear trend curves fitted.

In Figure 19, the South African data at 1880 m above sea level are compared with results from Calva et al [7]. The results of Calva et al [7] were obtained at 2240 m above sea level. For gap sizes between 200 mm and 600 mm, the South African results compare well with those of Calva [7], however, it again suggest lower flashover voltages for the longer gaps.

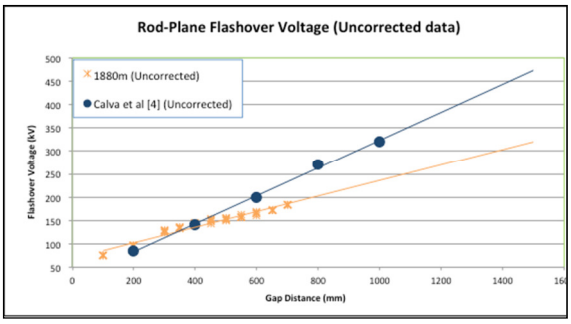


Figure 19: Comparison of the South African results (at 1800 m) to Calva [7] (with linear trend curves fitted).

Calva et al have on a number of occasions ([6] and [7]) stated that the IEC 60060-1 correction [3] is not valid for DC flashover voltages at high altitude.

7 CONCLUSIONS

The following conclusions were noted:

- Caution needs to be exercised when using IEC corrected test data from laboratories at low altitudes to predict DC flashover voltages at high altitudes.
- The South African results are in agreement with Calva et al [6],[7] that there are some discrepancies when using the IEC 60060-1:2010 correction [1] for DC voltages at high altitudes.
- The effect of other environmental variables such as wind and humidity on the flash-over voltage needs to be understood.
- To improve statistical confidence, more data taken at different altitudes is required to better understand the effect of altitude on the DC flashover voltage of a rod-plane gap. It would be necessary to get data at each if the measuring sites with approximately the same temperature and humidity, thus making altitude the only variable. This is achievable by undertaking a large number of measurements over a longer period (at each site) or developing a pressurised environmental chamber.
- The impact of altitude on the calculation of minimum safe live working clearances cannot be determined at this stage.

8 RECOMMENDATIONS

- It is recommended to repeat the measurements at each measuring site. To improve statistical confidence, more data per site is needed.
- It is recommended that two more test sites be used. These should be located at 1200 m and 600 m above sea level. This will allow for more accurate statistical analysis of the data.
- Larger air gaps need to be tested. This will only be possible if a higher voltage power supply is provisioned.

9 ACKNOWLEDGMENTS

The authors would like to acknowledge Mr A.C. Britten, and Mr C. Esterhuizen for their assistance and expert guidance in conducting this research. The authors would also like to thank Eskom for the support of this work and the High Voltage Engineering Research Group at the University of Witwatersrand, Johannesburg through the TESP programme. They would also like to thank the department of Trade and Industry (DTI-THRIP) as well as to the National Research Foundation (NRF) for direct funding of the High Voltage Engineering Research Group at the University of Witwatersrand, Johannesburg.

10 REFERENCES

[1] Parus N, Jandrell I.R, Reynders J.P, Mahatho N, Govender T, Roets H.A., “Preliminary results of an investigation into the effects of floating objects on the electrical breakdown of air under high voltage direct current stress”, 17th International Symposium on High Voltage Engineering, Hannover, Germany, August, 2011.

[2] Kuffel E, Zaengl W.S, Kuffel J, “High Voltage Engineering Fundamentals 2nd Edition”, Butterwort-Heinemann Publications, ISBN 0 7506 3634 3, Great Britain, 2000.

[3] International Electrotechnical Commission, “South African National Standard, High-voltage test techniques, Part 1: General definitions and test requirements”, SANS 60060 - 1:2011, IEC 60060 - 1:2010.

[4] Allen N.L, Boutlendj M, Lightfoot H.A, “Dielectric break down in non-uniform field air gaps”’, IEEE Transactions on Electrical Insulation, Volume: 28 , Issue: 2, Pages: 183 – 191, 1993.

[5] Udo T, Watanabe Y, “DC High-Voltage Sparkover Characteristics of Gaps and Insulator Strings”, IEEE Transactions on Power Apparatus and Systems, Volume: PAS-87, Issue: 1, Pages: 266 – 270, Jan. 1968.

[6] Calva P.A, Moral V. Del, Márquez M.G, Cabrera G.P, “New proposal of correction factors for dc voltages”, Conference on Electrical Insulation and Dielectric

Phenomena, 2003. Annual Report, 2003, Page(s): 455 – 458.
[7] Calva P.A, Espino F.P, “Correction factors for positive dc voltages”, IEEE Transactions on Dielectrics and Electrical Insulation, Volume: 5, 1998, Page(s): 541 – 544.